The Inflation Technique for Causal Inference with Latent Variables

Elie Wolfe,[1,*] Robert W. Spekkens,[1,†] and Tobias Fritz[1,2,‡]

[1] *Perimeter Institute for Theoretical Physics, Waterloo, Ontario, Canada, N2L 2Y5*
[2] *Max Planck Institute for Mathematics in the Sciences, Leipzig, Germany*

(Dated: August 16, 2016)

The fundamental problem of causal inference is to determine whether or not a given probability distribution over observed variables is compatible with some causal structure (which may incorporate latent variables). It is therefore valuable to be able to derive inequalities whose violation by a distribution witnesses the incompatibility of that distribution with the given causal structure. We term these causal compatibility inequalities. Prominent examples are Bell inequalities and Pearl's instrumental inequality. We here introduce a technique for deriving such inequalities for arbitrary causal structures. It consists of *inflating* the causal structure of interest to a new causal structure that can contain multiple copies of each of the original variables. By construction, any causal compatibility inequality on the inflated structure can be translated into one for the original structure. Because inflation often introduces novel d-separation relations, it often generates easy opportunities for such translations. We demonstrate the technique's power by numerically deriving all of the constraints that it implies for a particular concrete example—an inflation of the so-called triangle scenario —obtaining a set of causal compatibility inequalities that are provably stronger than those derived from other techniques. Given a *specific* probability distribution and a causal structure, our technique provides an efficient means of witnessing their incompatibility. Finally, we discuss how to identify, among the causal compatibility inequalities that the technique yields, those that remain necessary conditions on compatibility even for quantum (and post-quantum) generalizations of the notion of a causal model.

* ewolfe@perimeterinstitute.ca
† rspekkens@perimeterinstitute.ca
‡ fritz@mis.mpg.de

CONTENTS

I. INTRODUCTION

Given a joint probability distribution of some observed variables, the problem of **causal inference** is to determine which hypotheses about the causal mechanism can explain the given distribution. Here, a causal mechanism may comprise both causal relations among the observed variables, as well as among these and a number of unobserved variables. Causal inference problems arise in a wide variety of scientific disciplines, from sussing out biological pathways to enabling machine learning [1–4]. A closely related type of problem is to determine, for a given set of causal relations, the set of all distributions of observed variables that can be generated from them. A special case of both problems is the following decision problem: given a probability distribution and a hypothesis about the causal relations, determine whether the two are compatible—could the given distribution have been generated by the hypothesized causal relations? This is the problem that we focus on. We develop necessary conditions for a given distribution to be compatible with a given hypothesis about the causal relations.

In the simplest setting, the causal hypothesis consists of a directed acyclic graph (DAG) *all* of whose nodes correspond to observed variables. In this case, obtaining a verdict on the compatibility of a given distribution with the causal hypothesis is simple: the compatibility holds if and only if the distribution is Markov with respect to the DAG, which is to say that the distribution features all of the conditional independence relations asserted by d-separation with respect to the DAG. The compatible DAGs can be determined algorithmically solely from the distribution [1].

A significantly more difficult case is when one considers a causal hypothesis which consists of a DAG whose nodes include **latent** (i.e., unobserved) variables, so that the set of observed variables is a strict subset of the nodes of the DAG. This case occurs, e.g., in situations where one needs to deal with the possible presence of unobserved confounders, and is particularly relevant for experimental design in statistics.

It is useful to distinguish two varieties of this problem: (i) the causal hypothesis specifies that the latent variables are discrete and of a particular cardinality[1], and (ii) the nature of the latent variables is arbitrary.

Consider the first variety of causal inference problem, where the cardinalities of all the latent variables are finite. Then the mathematical problem which one must solve to infer the distributions that are compatible with the hypothesis is a quantifier elimination problem for some finite number of quantifiers, as follows. The probabilities making up the distribution over the observed variables can all be expressed as functions of the parameters specifying the conditional probabilities of each node given its parents, many of which involve latent variables. If one can eliminate these parameters, then one obtains constraints that refer exclusively to the probability distribution of the observed variables. This is a *nonlinear* quantifier elimination problem. While the Tarski-Seidenberg theorem provides an *in principle* algorithm for an exact solution, the computational complexity of such quantifier elimination techniques is too large to be practical, except in particularly simple scenarios [5]. Techniques for finding approximate solutions to nonlinear quantifier elimination may help [6].

The second variety of causal inference problem, where the latent variables are arbitrary, is even more difficult, but it is the one that has been the focus of most research and that motivates the present work. It is conceivable that inference problems of this variety can be expressed as quantifier elimination problems as well. This would be the case, for instance, if one could show that latent variables of a certain finite cardinality (as opposed to arbitrary latent variables) are sufficient to generate all the distributions compatible with a given DAG[2]. At present, however, the problem of finding an algorithm for deciding compatibility in this second case—let alone an efficient algorithm—remains open. Nonetheless, even if it *is* possible to achieve a reduction to the case of latent variables with finite cardinality, one would still be faced with a computationally impractical nonlinear quantifier elimination problem, as described above. As such, a heuristic technique for obtaining nontrivial constraints, such as the one presented in this work, is arguably more useful.

If one allows for latent variables, then the condition that all of the conditional independence relations among the observed variables should be explained by the structure of the DAG is still a necessary condition for compatibility of a DAG with a given distribution, but in general it is no longer a sufficient condition for compatibility. Historically, the insufficiency of the conditional independence relations for causal inference in the presence of latent variables was first noted by Bell in the context of the hidden variable problem in quantum physics [8]. Bell considered an experiment for which considerations from relativity theory implied a very particular causal structure, and he derived an inequality that any distribution compatible with this structure, and compatible with certain constraints imposed by quantum theory, must satisfy. Bell also showed that this inequality was violated by distributions generated from entangled quantum states with particular choices of incompatible measurements. Later work, by Clauser, Horne, Shimony and Holte (CHSH) [9] showed how to derive inequalities directly from the causal structure. The CHSH inequality was the first example of a compatibility condition that appealed to the strength of the correlations rather than simply the conditional independence relations inherent therein. Since then, many generalizations of the CHSH inequality have been derived for the same sort of causal structure [10]. The idea that such work is best understood as a contribution to the field of causal inference has only recently been put forward [11–14], as has the idea that techniques developed by researchers in the foundations of quantum theory may be usefully adapted to causal inference[3].

Subsequent to Bell's work, Pearl derived an inequality, called the **instrumental inequality** [22], which provides a necessary condition for the compatibility of a distribution with a causal structure known as the *instrumental scenario*. This causal structure is applicable, for instance, to certain kinds of noncompliance in drug trials. Steudel and Ay [23] later derived an inequality which must hold whenever a distribution on n variables is compatible with a causal structure where no set of more than c variables has a common ancestor, for arbitrary $n, c \in \mathbb{N}$. Subsequent work has focused specifically on the case of $n = 3$ and $c = 2$, a causal structure that has been called the Triangle scenario [12, 24].

Recently, Henson, Lal and Pusey [13] have found a sufficient condition for a DAG to be *interesting*, by which they mean that conditional independence relations do not exhaust the set of constraints on the compatibility of a joint distribution over observed variables with the DAG. They also presented a catalogue of all potentially interesting DAGs having six or fewer nodes in [13, App. E], of which all but three were shown to be indeed interesting. The Bell scenario, the Instrumental scenario, and the Triangle scenario appear in the catalogue together with many others. Furthermore, the fraction of DAGs that are interesting increases as the total number of nodes increases. This highlights the need for moving beyond a case-by-case consideration of individual DAGs and for developing techniques for deriving

[1] The cardinality of a variable is the number of possible values it can take.

[2] Rosset and Gisin [7] have an unpublished proof purporting to upper bound the cardinality of the latent variables for a particular DAG. We do not pursue the question here.

[3] The current article being another example of the phenomenon [6, 15–21].

constraints beyond conditional independence relations that can be applied to any interesting DAG. Shannon-type entropic inequalities are an example of such constraints [12, 16, 23–25]. They can be derived for a given DAG with relative ease, via exclusively linear quantifier elimination, since conditional independence relations are linear equations at the level of entropies. They also have the advantage that they apply regardless of the cardinality of the observable variables. Recent work has also looked at non-Shannon type inequalities, potentially further strengthening the entropic constraints [17, 26]. However, entropic techniques are still wanting, since the resulting inequalities are often rather weak. For example, they are not sensitive enough to distinguish uniquely-quantum correlations from their classical causal counterparts [12, 17][4].

We here introduce a new technique for deriving necessary conditions for the compatibility of a distribution over observed variables with a given causal structure, which we term the *inflation technique*. Our technique is frequently capable of witnessing incompatibility when many other causal inference techniques fail. For example, in Example 2 of Sec. III-B we prove that the tripartite "W-type" distribution is incompatible with the Triangle scenario, despite the incompatibility being invisible to other causal inference tools such as conditional independence relations, Shannon-type [16, 24, 25] or non-Shanon-type entropic inequalities [17], or covariance matrices [18].

The inflation technique works roughly as follows. For a given DAG under consideration, one can construct many new DAGs, termed *inflations* of this DAG. These duplicate one or more of the nodes of the original DAG, while preserving the subgraph describing their ancestry. Furthermore, the causal parameters that one adds to the inflated DAG are constrained to mirror those of the original DAG. We show that if the distributions over certain subsets of the observed variables are compatible with the original DAG, then the same distributions over certain copies of those subsets in the inflated DAG are compatible with the inflated DAG. Similarly, we show that any necessary condition for compatibility of a distribution with the inflated DAG translates into a necessary condition for compatibility with the original DAG. Thus standard techniques for deriving inequalities, applied to the inflated DAG, can be supplemented with the inflation technique to derive new inequalities for the original DAG. Concretely, we consider inequalities on the inflated DAG that are obtained from the *mere existence of a joint distribution* on the inflated DAG, supplemented with independence constraints arising from the inflated causal structure. We show how to derive a complete set of such inequalities by enumerating all facets of the associated **marginal polytope**. We also show how to compute a partial solution more efficiently by enumerating transversals of a certain hypergraph. Translating these back to the original DAG results in causal compatibility conditions in the form of nonlinear *polynomial inequalities*.

Besides the entropic techniques discussed above, our method is the first systematic tool for causal inference with latent variables that goes beyond observable conditional independence relations while not assuming any bounds on the cardinality of each latent variable. While our method can be used to systematically generate necessary conditions for compatibility with a given causal structure, we do not know whether the set of inequalities thus generated are also sufficient.

While we present our technique primarily as a tool for standard causal inference, we also briefly discuss applications to *quantum* causal models and causal models within generalized probabilistic theories [12–14, 16]. In particular, we discuss when our inequalities are also necessary conditions for a distribution over observed variables to be compatible with a given DAG within any generalized probabilistic theory.

II. BASIC DEFINITIONS OF CAUSAL MODELS AND COMPATIBILITY

A **causal model** consists of a pair of objects: a **causal structure** and a set of **causal parameters**. We define each in turn. Recall the definition of a directed acyclic graph (DAG). A DAG G consists of a finite set of nodes $\mathsf{Nodes}[G]$ and a set of directed edges $\mathsf{Edges}[G]$, where a directed edge is an ordered pair of nodes. In the context of a causal model, each node carries a random variable and a directed edge between two nodes corresponds to the possibility of a direct causal influence from one variable to the other. In this way, the edges implement causal relations.

Our terminology for the causal relations between the nodes in a DAG is the standard one. The parents of a node X in G are defined as those nodes from which an outgoing edge terminates at X, i.e. $\mathsf{Pa}_G(X) = \{ Y \mid Y \to X \}$. When the graph G is clear from the context, then we also omit the subscript. Similarly, the children of a node X in a given graph G are defined as those nodes at which edges originating at X terminate, i.e. $\mathsf{Ch}_G(X) = \{ Y \mid X \to Y \}$. If $\boldsymbol{U}$ is a set of nodes, then we put $\mathsf{Pa}_G(\boldsymbol{U}) := \bigcup_{X \in \boldsymbol{U}} \mathsf{Pa}_G(X)$ and $\mathsf{Ch}_G(\boldsymbol{U}) := \bigcup_{X \in \boldsymbol{U}} \mathsf{Ch}_G(X)$. The **ancestors** of a set of nodes $\boldsymbol{U}$, denoted $\mathsf{An}_G(\boldsymbol{U})$, are defined as those nodes which have a directed *path* to some node in $\boldsymbol{U}$, *including the*

[4] It should be noted that non-standard entropic inequalities can be obtained through a fine-graining of the causal scenario, namely by *conditioning* on the distinct finite possible outcomes of root variables ("settings"), and these types of inequalities *have* proven somewhat quantum-sensitive [24, 27, 28]. Such inequalities are still limited, however, in that they are only applicable to those DAGs which feature observable root nodes. The potential utility of entropic analysis where fine-graining is generalized to *non*-root observable nodes is currently being explored by E.W. and Rafael Chaves. Jacques Pienaar has also alluded to similar considerations as a possible avenue for further research [26].

nodes in $\boldsymbol{U}$ *themselves*[5]. Equivalently, $\mathsf{An}(\boldsymbol{U}) := \bigcup_{n\in\mathbb{N}} \mathsf{Pa}^n(\boldsymbol{U})$, where $\mathsf{Pa}^n(\boldsymbol{U})$ is inductively defined via $\mathsf{Pa}^0(\boldsymbol{U}) := \boldsymbol{U}$ and $\mathsf{Pa}^{n+1}(\boldsymbol{U}) := \mathsf{Pa}(\mathsf{Pa}^n(\boldsymbol{U}))$.

A **causal structure** is a DAG G that incorporates a distinction between two types of nodes: the set of observed nodes $\mathsf{ObservedNodes}[G]$, and the set of latent nodes $\mathsf{LatentNodes}[G]$. Following [13], we will depict the observed nodes by triangles and the latent nodes by circles, as in Fig. 1. Henceforth, we will use the terms "DAG" and "causal structure" interchangeably, so that the specification of which variables are observed is considered to be part of the DAG. We denote the variable living at a node $X \in \mathsf{Nodes}[G]$ by the same letter X. Frequently we supplement the causal structure by a specification of the cardinalities of the observed variables.

The second component of a causal model is a set of **causal parameters**.The set of causal parameters specifies, for each node X, the conditional probability distribution over the values of the random variable X, given the values of the variables $\mathsf{Pa}(X)$. In the case of root nodes, we have $\mathsf{Pa}(X) = \emptyset$, and the conditional distribution is an unconditioned distribution. We write $P_{Y|X}$ for the conditional distribution of a variable Y given a variable X, while the particular conditional probability of the variable X taking the value x given that the variable Y takes the values y is denoted[6] $P_{Y|X}(y|x)$. Therefore, a given set of causal parameters has the form

$$\{P_{A|\mathsf{Pa}_G(A)} : A \in \mathsf{Nodes}[G]\}. \tag{1}$$

Finally, a **causal model** M consists of a causal structure together with a set of causal parameters,

$$M = (G, \{P_{A|\mathsf{Pa}_G(A)} : A \in \mathsf{Nodes}[G]\}).$$

A causal model specifies a joint distribution over all variables in the DAG via

$$P_{\mathsf{Nodes}[G]} = \prod_{A\in\mathsf{Nodes}[G]} P_{A|\mathsf{Pa}_G(A)}, \tag{2}$$

where $\prod$ denotes the usual product of functions, so that $(P_X \times P_Y)(x, y) := P_X(x)P_Y(y)$. A distribution $P_{\mathsf{Nodes}[G]}$ arises in this way if and only if it satisfies the Markov conditions associated to G.

The joint distribution over the observed variables is obtained from the joint distribution over all variables by marginalization over the latent variables

$$P_{\mathsf{ObservedNodes}[G]} = \sum_{\{X:X\in\mathsf{LatentNodes}[G]\}} P_{\mathsf{Nodes}[G]}, \tag{3}$$

where $\sum_X$ denotes marginalization over the variable X, so that $(\sum_X P_{XY})(y) := \sum_x P_{XY}(xy)$.

A given distribution of observed variables is said to be **compatible** with a given causal structure if there is some choice of the causal parameters that yields the given distribution via Eqs. (2) and (3). Furthermore, a given set of marginal distributions of various subsets of observed variables is said to be compatible with a given causal structure if and only if there exists a joint distribution of observed variables that yields these marginals and is compatible with the causal structure.

III. THE INFLATION TECHNIQUE FOR CAUSAL INFERENCE

A. Inflations of a causal model

We now introduce the notion of **an inflation of a causal model**. If a causal model lives on a DAG G, then an inflation of this model lives on an **inflation DAG** G'. There are many possible choices of inflation DAGs G' for a given G, forming a set $\mathsf{Inflations}[G]$. The choice of $G' \in \mathsf{Inflations}[G]$ is the only freedom in the inflation of a causal model. Once a choice is made, the set of parameters of the inflated model M' is fixed uniquely by the set of parameters of the original model M by a function $M' = \mathsf{Inflation}_{G\to G'}[M]$ that we define below. We begin by defining the condition under which a DAG G' is an inflation of a DAG G. This requires some preliminary definitions.

The **induced subgraph** of G obtained by restricting to a subset of nodes $\boldsymbol{V} \subseteq \mathsf{Nodes}[G]$ will be denoted $\mathsf{SubDAG}_G(\boldsymbol{V})$. It consists of the nodes $\boldsymbol{V}$ and those edges of G of which both endpoints are in $\boldsymbol{V}$. Of special

[5] Note that this inclusion of a node within the set of its ancestors is contrary to the colloquial use of the term "ancestors". We use this definition so that any correlation between two variables can always be attributed to a common "ancestor". This includes, for instance, the case where one variable is the parent of the other.

[6] Although our notation suggests that all variables are discrete, we do not make this assumption. All of our equations are straightforward to write down with proper measure-theoretic notation.

importance to us is the **ancestral subgraph** of $\boldsymbol{V}$, denoted $\mathsf{AnSubDAG}_G(\boldsymbol{V})$, which is the subgraph induced by the ancestry of $\boldsymbol{V}$, $\mathsf{AnSubDAG}_G(\boldsymbol{V}) \coloneqq \mathsf{SubDAG}_G(\mathsf{An}_G(\boldsymbol{V}))$.

In an inflation DAG G', every node behaves like a copy of a node of G. More precisely, the structure of being an inflation DAG also comprises a map $G' \to G$. We call the preimages of a node $A \in \mathsf{Nodes}[G]$ the *copies* of A in G', and denote them by $A_1, \ldots, A_k$. The subscript that indexes the copies is termed the **copy-index**. When two objects (e.g. nodes, sets of nodes, DAGs, etc…) are the same up to copy-indices, then we use $\sim$ to indicate this, as in $A_i \sim A_j \sim A$. Other examples are that $\boldsymbol{U} \sim \boldsymbol{U'}$ for sets of nodes $\boldsymbol{U} \subseteq \mathsf{Nodes}[G]$ and $\boldsymbol{U}' \subseteq \mathsf{Nodes}[G']$ if and only if $\boldsymbol{U'}$ contains exactly one copy of every node in $\boldsymbol{U}$, and similarly $\mathsf{SubDAG}_{G'}(\boldsymbol{U}') \sim \mathsf{SubDAG}_G(\boldsymbol{U})$ means in addition that an edge is present between two nodes in $\boldsymbol{U}'$ if and only if it is present between the two associated nodes in $\boldsymbol{U}$.

In order to be an inflation, G' must locally mirror the causal structure of G:

Definition 1. *The DAG G' is said to be an **inflation** of the DAG G, that is, $G' \in \mathsf{Inflations}[G]$, if and only if for every node A_i in G', the ancestral subgraph of A_i in G' is equivalent, under removal of the copy-index, to the ancestral subgraph of A in G,*

$$G' \in \mathsf{Inflations}[G] \quad \textit{iff} \quad \forall A_i \in \mathsf{Nodes}[G'] : \ \mathsf{AnSubDAG}_{G'}(A_i) \sim \mathsf{AnSubDAG}_G(A). \tag{4}$$

To illustrate the notion of inflation, we consider the DAG of Fig. 1, which is called the *Triangle scenario* (for obvious reasons) and which has been studied by many authors [13 (Fig. E#8), 11 (Fig. 18b), 12 (Fig. 3), 24 (Fig. 6a), 29 (Fig. 1a), 30 (Fig. 8), 23 (Fig. 1b), 16 (Fig. 4b)]. Different inflations of the Triangle scenario are depicted in Figs. 2 to 6, which, for ease of reference, will be referred to as the *web*, *spiral*, *capped*, and *cut* inflations respectively.

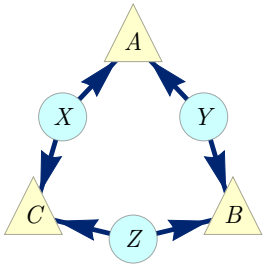

FIG. 1. The Triangle scenario.

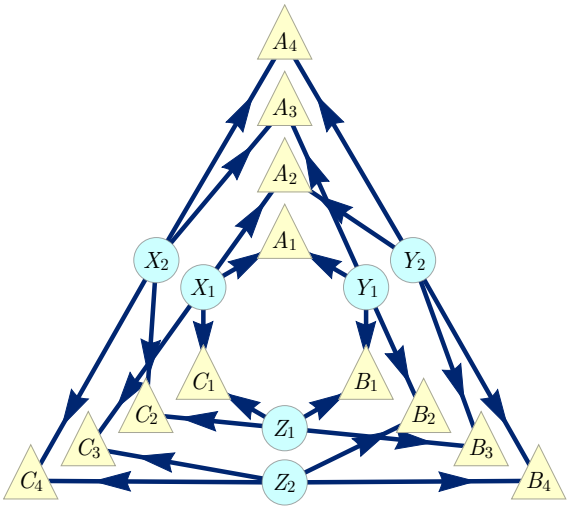

FIG. 2. The web inflation of the Triangle scenario where each latent node has been duplicated and each observable node has been quadrupled. The four copies of each observed node correspond to the four possible choices of parentage given the pair of copies of each latent parent of the observed node.

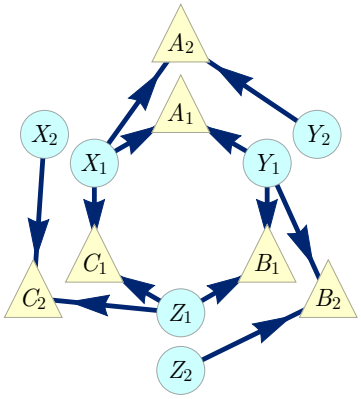

FIG. 3. The spiral inflation of the Triangle scenario. Notably, this DAG is the ancestral subgraph of the set $\{A_1A_2B_1B_2C_1C_2\}$ in the web inflation (Fig. 2).

We now define the function $\mathsf{Inflation}_{G\to G'}$, that is, we specify how the causal parameters are defined for a given inflation DAG

Definition 2. *Consider causal models M and M' where $\mathsf{DAG}[M] = G$ and $\mathsf{DAG}[M'] = G'$ and such that G' is an inflation of G. The causal model M' is said to be the $G \to G'$ **inflation of** M, that is, $M' = \mathsf{Inflation}_{G\to G'}[M]$, if and only if for every node A_i in G', the manner in which A_i depends causally on its parents within G' is the same as the manner in which A depends causally on its parents within G. Noting that $A_i \sim A$ and that $\mathsf{Pa}_{G'}(A_i) \sim \mathsf{Pa}_G(A)$ by Eq. (4), one can formalize this condition as:*

$$\forall A_i \in \mathsf{Nodes}[G'] : \ P_{A_i|\mathsf{Pa}_{G'}(A_i)} = P_{A|\mathsf{Pa}_G(A)}. \tag{5}$$

It is clear that for a given triple G, G', and M, this definition specifies a unique inflation model M', resulting in a well-defined function $\mathsf{Inflation}_{G\to G'}$.

To sum up then, the inflation of a causal model is a new causal model where (i) each variable in the original DAG may have counterparts in the inflated DAG with ancestral subgraphs mirroring those of the originals, and (ii) the manner in which a variable depends causally on its parents in the inflated DAG is given by the manner in which its counterpart in the original DAG depends causally on its parents. The operation of modifying a DAG and equipping the modified version with conditional probability distributions that mirror those of the original also appears in the *do calculus* and *twin networks* of Pearl [1], and moreover bears some resemblance to the *adhesivity* technique used in deriving non-Shannon-type entropic inequalities (Appendix D).

We are now in a position to describe the key property of the inflation of a causal model, the one that makes it useful for causal inference. With notation as in Definition 2, let $P_{\boldsymbol{U}}$ and $P_{\boldsymbol{U}'}$ denote marginal distributions on some sets of nodes $\boldsymbol{U} \subseteq \mathsf{Nodes}[G]$ and $\boldsymbol{U}' \subseteq \mathsf{Nodes}[G']$, respectively. Then

$$\text{if} \quad \boldsymbol{U}' \sim \boldsymbol{U} \;\text{ and }\; \mathsf{AnSubDAG}_{G'}(\boldsymbol{U}') \sim \mathsf{AnSubDAG}_{G}(\boldsymbol{U}), \quad \text{then} \quad P_{\boldsymbol{U}'} = P_{\boldsymbol{U}}. \tag{6}$$

This follows from the fact that the probability distributions over $\boldsymbol{U}'$ and $\boldsymbol{U}$ depend only on their ancestral subgraphs and the parameters defined thereon, which by the definition of inflation are the same for $\boldsymbol{U}'$ and for $\boldsymbol{U}$. It is useful to have a name for those sets of observed nodes in G' which satisfy the antecedent of Eq. (6), that is, for which one can find a copy-index-equivalent set in the original DAG G with a copy-index-equivalent ancestral subgraph. We call such subsets of the observed nodes of G' **injectable sets**,

$$\begin{aligned} &\boldsymbol{U}' \in \mathsf{InjectableSets}[G'] \\ &\quad \text{iff} \quad \exists \boldsymbol{U} \subseteq \mathsf{ObservedNodes}[G] \;:\; \boldsymbol{U}' \sim \boldsymbol{U} \;\text{ and }\; \mathsf{AnSubDAG}_{G'}(\boldsymbol{U}') \sim \mathsf{AnSubDAG}_{G}(\boldsymbol{U}). \end{aligned} \tag{7}$$

Similarly, those sets of observed nodes in the original DAG G which satisfy the antecedent of Eq. (6), that is, for which one can find a corresponding set in the inflated DAG G' with a copy-index-equivalent ancestral subgraph, we describe as **images of the injectable sets**,

$$\begin{aligned} &\boldsymbol{U} \in \mathsf{ImagesInjectableSets}[G] \\ &\quad \text{iff} \quad \exists \boldsymbol{U}' \subseteq \mathsf{ObservedNodes}[G'] \;:\; \boldsymbol{U}' \sim \boldsymbol{U} \;\text{ and }\; \mathsf{AnSubDAG}_{G'}(\boldsymbol{U}') \sim \mathsf{AnSubDAG}_{G}(\boldsymbol{U}). \end{aligned} \tag{8}$$

Clearly, $\boldsymbol{U} \in \mathsf{ImagesInjectableSets}[G]$ iff $\exists \boldsymbol{U}' \subseteq \mathsf{InjectableSets}[G']$ such that $\boldsymbol{U} \sim \boldsymbol{U}'$.

For example in the inflation of the Triangle scenario depicted in Fig. 3, the set of observed nodes $\{A_1B_1C_1\}$ is injectable because its ancestral subgraph is equivalent up to copy-indices to the ancestral subgraph of $\{ABC\}$ in the original DAG, and the set $\{A_2C_1\}$ is injectable because its ancestral subgraph is equivalent to that of $\{AC\}$ in the original DAG.

A set of nodes in the inflated DAG can only be injectable if it contains at most one copy of any node from the original DAG. More strongly, it can only be injectable if its ancestral subgraph contains at most one copy of any

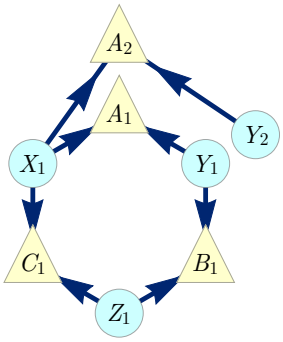

FIG. 4. The capped inflation of the Triangle scenario; notably also the ancestral subgraph of the set $\{A_1A_2B_1C_1\}$ in the spiral inflation (Fig. 3).

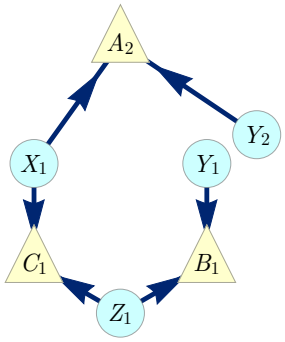

FIG. 5. The cut inflation of the Triangle scenario; notably also the ancestral subgraph of the set $\{A_2B_1C_1\}$ in the capped inflation (Fig. 4). Note that, unlike the other examples, this inflation does not contain the Triangle scenario as a subgraph.

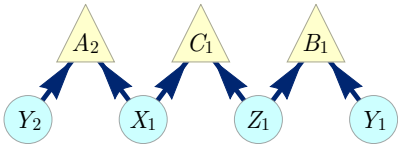

FIG. 6. A different depiction of the cut inflation of Fig. 5.

node from the original DAG. Thus, in Fig. 3, $\{A_1A_2C_1\}$ is not injectable because it contains two copies of A, and $\{A_2B_1C_1\}$ is not injectable because its ancestral subgraph contains two copies of Y.

The fact that the sets $\{A_1B_1C_1\}$ and $\{A_2C_1\}$ are injectable implies, via Eq. (6), that the marginals on each of these in the inflation model are precisely equal to the marginals on their counterparts, $\{ABC\}$ and $\{AC\}$, in the original causal model, so that $P_{A_1B_1C_1} = P_{ABC}$ and $P_{A_2C_1} = P_{AC}$.

It is useful to express Eq. (6) in the language of injectable sets,

$$P_{\boldsymbol{U}'} = P_{\boldsymbol{U}} \quad \text{if} \quad \boldsymbol{U}' \sim \boldsymbol{U} \ \text{ and } \ \boldsymbol{U}' \in \mathsf{InjectableSets}[G']. \tag{9}$$

B. Witnessing incompatibility

Finally, we can explain why inflation is relevant for deciding whether a distribution is compatible with a causal structure. For a family of marginal distributions $\{P_{\boldsymbol{U}} : \boldsymbol{U} \in \mathsf{ImagesInjectableSets}[G]\}$ to be compatible with G, there must be a causal model M that yields a joint distribution with this family as its marginals. Looking at the inflation model $M' = \mathsf{Inflation}_{G\to G'}[M]$, Eq. (9) implies that M' has the corresponding family of marginals given by $\{P_{\boldsymbol{U}'} : \boldsymbol{U}' \in \mathsf{InjectableSets}[G']\}$ with $P_{\boldsymbol{U}'} = P_{\boldsymbol{U}}$ for $\boldsymbol{U}' \sim \boldsymbol{U}$, and thus this family is compatible with G'.

The same considerations apply for any collection of injectable sets:

Lemma 3. *Let G' be an inflation DAG of G. Let $S' \subseteq \mathsf{InjectableSets}[G']$ be a collection of injectable sets, and let $S \subseteq \mathsf{ImagesInjectableSets}[G]$ be the images of this collection. If the family of marginal distributions $\{P_{\boldsymbol{U}} : \boldsymbol{U} \in S\}$ is compatible with G, then the corresponding family of marginal distributions $\{P_{\boldsymbol{U}'} : \boldsymbol{U}' \in S'\}$ — defined via $P_{\boldsymbol{U}'} = P_{\boldsymbol{U}}$ for $\boldsymbol{U}' \sim \boldsymbol{U}$ — is compatible with G'.*

We have thereby related a question about compatibility with the original causal structure to one about compatibility with the inflated causal structure. If one can show that the new compatibility question on G' is answered in the negative, then one can infer that the original question is answered in the negative as well. Some simple examples serve to illustrate the idea.

Example 1. **Witnessing the incompatibility of perfect three-way correlation with the Triangle scenario.**

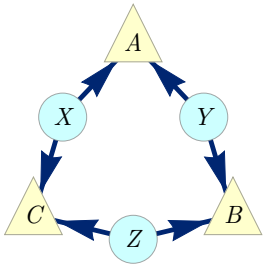

FIG. 7. The Triangle scenario. (Repeat of Fig. 1.)

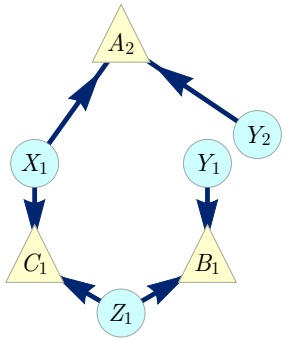

FIG. 8. The cut inflation of the Triangle scenario. (Repeat of Fig. 5.)

Consider the following causal inference problem. One is given a joint distribution over three binary variables, P_{ABC}, where the marginal on each variable is uniform and the three are perfectly correlated,

$$P_{ABC} = \frac{[000] + [111]}{2}, \quad \text{i.e.,} \quad P_{ABC}(abc) = \begin{cases} \frac{1}{2} & \text{if } a{=}b{=}c, \\ 0 & \text{otherwise,} \end{cases} \tag{10}$$

and one would like to determine whether it is compatible with the Triangle scenario, that is, the DAG depicted in Fig. 7. The notation $[abc]$ in Eq. (10) is shorthand for the point distribution where A, B, and C take the values a, b, and c respectively; in terms of the Kronecker-delta function, $[abc] := \delta_{A,a}\delta_{B,b}\delta_{C,c}$,

Since there are no conditional independence relations among the observed variables in the Triangle scenario, there is no opportunity for ruling out the distribution on the grounds that it fails to satisfy the required conditional independences.

To solve this problem, we consider the cut inflation of the Triangle scenario, depicted in Fig. 8. The injectable sets in this case include $\{A_2C_1\}$ and $\{B_1C_1\}$. Their images on the original DAG are $\{AC\}$ and $\{BC\}$ respectively.

We will show that the distribution of Eq. (10) is not compatible with the Triangle scenario by demonstrating that the contrary assumption of compatibility implies a contradiction.

If the distribution of Eq. (10) is compatible with the Triangle scenario, then so are its marginals on $\{AC\}$ and $\{BC\}$, which are given by:

$$P_{AC} = P_{BC} = \frac{[00] + [11]}{2}.$$

From the definition of inflation, together with the fact that $\{A_2C_1\}$ and $\{B_1C_1\}$ are injectable sets whose images on the original DAG are $\{AC\}$ and $\{BC\}$, we can infer that if the marginals P_{AC} and P_{BC} are compatible with the Triangle scenario, then the marginals

$$P_{A_2C_1} = P_{B_1C_1} = \frac{[00] + [11]}{2}.$$

are compatible with the cut inflation of the Triangle scenario. This is the specialization of Lemma 3 to this example.

Finally, we show that the pair of marginals $P_{A_2C_1}$ and $P_{B_1C_1}$ are *not* compatible with the cut inflated DAG, thereby obtaining our contradiction. It suffices to note that (i) the only joint distribution that exhibits perfect correlation between A_2 and C_1 and between B_1 and C_1 also exhibits perfect correlation between A_2 and B_1, and (ii) A_2 and B_1 have no common ancestors in the cut inflated DAG and hence must be marginally independent in any distribution that is compatible with it.

We have therefore certified that the joint distribution P_{ABC} of Eq. (10) is not compatible with the Triangle causal structure, recovering a result originally proven by Steudel and Ay [23].

Example 2. **Witnessing the incompatibility of the W-type distribution with the Triangle scenario.**

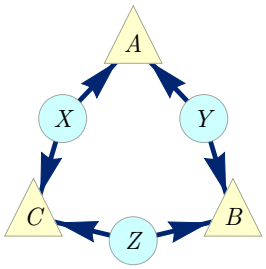

FIG. 9. The Triangle scenario. (Repeat of Fig. 1.)

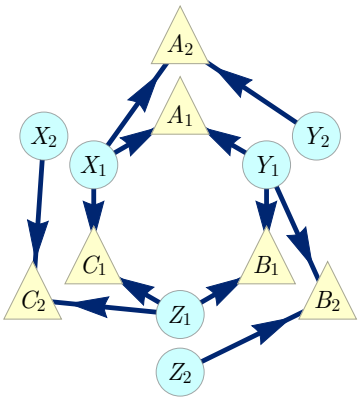

FIG. 10. The spiral inflation of the Triangle scenario. (Repeat of Fig. 3.)

Consider another causal inference problem concerning the Triangle scenario, namely, that of determining whether the hypothesis of the Triangle DAG is compatible with a joint distribution P_{ABC} of the form

$$P_{ABC} = \frac{[100] + [010] + [001]}{3}, \quad \text{i.e.,} \quad P_{ABC}(abc) = \begin{cases} \frac{1}{3} & \text{if } a{+}b{+}c{=}1, \\ 0 & \text{otherwise.} \end{cases} \tag{11}$$

We call this the W-type distribution[7].

To settle the compatibility question, we consider the spiral inflation of the Triangle scenario (Fig. 10). The injectable sets in this case include $\{A_1B_1C_1\}$, $\{A_2C_1\}$, $\{B_2A_1\}$, $\{C_2B_1\}$, $\{A_2\}$, $\{B_2\}$ and $\{C_2\}$.

[7] The name stems from the fact that this distribution is reminiscent of the quantum state appearing in [31], called the *W state*.

Therefore, we turn our attention to determining whether the marginals of the W-type distribution on the images of these injectable sets are compatible with the Triangle hypothesis. These marginals are:

$$P_{ABC} = \frac{[100] + [010] + [001]}{3}, \tag{12}$$

$$P_{AC} = P_{BA} = P_{CB} = \frac{[10] + [01] + [00]}{3}, \tag{13}$$

$$P_A = P_B = P_C = \frac{2}{3}[0] + \frac{1}{3}[1]. \tag{14}$$

But by Lemma 3, this compatibility holds only if the the equivalent marginals for the injectable sets, namely,

$$P_{A_1B_1C_1} = \frac{[100] + [010] + [001]}{3}, \tag{15}$$

$$P_{A_2C_1} = P_{B_2A_1} = P_{C_2B_1} = \frac{[10] + [01] + [00]}{3}, \tag{16}$$

$$P_{A_2} = P_{B_2} = P_{C_2} = \frac{2}{3}[0] + \frac{1}{3}[1]. \tag{17}$$

are compatible with the spiral inflation of the Triangle scenario (Fig. 10).

Eq. (16) implies that C_1=0 whenever A_2=1. It also implies that A_1=0 whenever B_2=1, and that B_1=0 whenever C_2=1,

$$\begin{aligned} A_2{=}1 &\implies C_1{=}0, \\ B_2{=}1 &\implies A_1{=}0, \\ C_2{=}1 &\implies B_1{=}0. \end{aligned} \tag{18}$$

Our inflated DAG is such that A_2, B_2 and C_2 have no common ancestor and consequently are marginally independent in any distribution consistent with this inflated DAG. This fact, together with Eq. (17), implies that

$$\text{Sometimes} \quad A_2{=}1 \text{ and } B_2{=}1 \text{ and } C_2{=}1. \tag{19}$$

Finally, Eq. (18) together with Eq. (19) entails

$$\text{Sometimes} \quad A_1{=}0 \text{ and } B_1{=}0 \text{ and } C_1{=}0. \tag{20}$$

This, however, contradicts Eq. (15). Consequently, the set of marginals described in Eqs. (15-17) are *not* compatible with the DAG of Fig. 10. By Lemma 3, this implies that the set of marginals described in Eqs. (12-14)—and therefore the W-type distribution of which they are marginals—is not compatible with the Triangle scenario.

To our knowledge, this has not been demonstrated previously. In fact, the incompatibility of the W-type distribution with the Triangle scenario cannot be derived via any of the following pre-existing causal inference techniques:

1. Checking conditional independence relations is not relevant here, as there are *no* conditional independence relations implied between any observable variables in the Triangle scenario.
2. The relevant Shannon-type entropic inequalities for the Triangle scenario have been classified, and they do not witness the incompatibility either [16, 24, 25].
3. Moreover, *no* entropic inequality can witness the W-type distribution as unrealizable. Weilenmann and Colbeck [17] have constructed an inner approximation to the entropic cone of the Triangle causal structure, and the W-distribution lies inside this. In other words, a distribution with the same entropic profile as the W-type distribution *can* arise from the Triangle scenario.
4. The newly-developed method of covariance matrix causal inference due to Åberg *et al.* [18], which gives tighter constraints than entropic inequalities for the Triangle scenario, also cannot detect the incompatibility.

Therefore, for this problem at least, the inflation technique appears to be more powerful.

We have arrived at our incompatibility verdict by combining inflation with reasoning reminiscent of Hardy's version of Bell's theorem [32, 33]. Sec. IV-E will present a generalization of this kind of argument and its applications to causal inference.

Example 3. **Witnessing the incompatibility of PR-box correlations with the Bell scenario.**

Bell's theorem [8–10, 34] concerns the question of whether the distribution obtained in an experiment involving a pair of systems that are measured at space-like separation is compatible with a causal structure of the form of Fig. 11.

Here, the observed variables are $\{A, B, X, Y\}$, and Λ is a latent variable acting as a common cause of A and B. We shall term this causal structure the *Bell scenario*. While the causal inference formulation of Bell's theorem is not the traditional one, several recent articles have introduced and advocated this perspective [11 (Fig. 19), 13 (Fig. E#2), 14 (Fig. 1), 24 (Fig. 1), 35 (Fig. 2b), 36 (Fig. 2)].

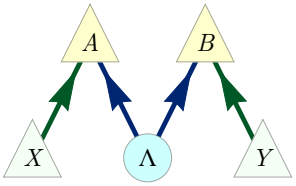

FIG. 11. The causal structure of the bipartite Bell scenario. The local outcomes A and B of Alice's and Bob's measurements is assumed to be a function of some latent common cause and their independent local experimental settings X and Y.

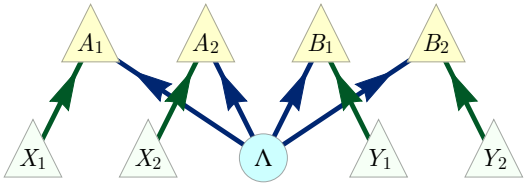

FIG. 12. An inflated DAG of the bipartite Bell scenario, where both local settings and outcome variables have been duplicated.

We consider the distribution $P_{ABXY} = P_{AB|XY} P_X P_Y$, where P_X and P_Y are arbitrary full-support distributions[8] over the binary variables X and Y, and

$$P_{AB|XY}(ab|xy) = \begin{cases} \frac{1}{2} & \text{if } \ a + b \equiv x \cdot y \pmod 2, \\ 0 & \text{otherwise,} \end{cases} \tag{21}$$

a conditional distribution that was discovered by Tsirelson [37] and later independently by Popescu and Rohrlich [38, 39]. It has become known in the field of quantum foundations as the *PR-box* after the latter authors.[9]

The Bell scenario implies nontrivial conditional independences[10] among the observed variables, namely, $X \perp\!\!\!\perp Y$, $A \perp\!\!\!\perp Y|X$, and $B \perp\!\!\!\perp X|Y$, as well as those that can be generated from these by the semi-graphoid axioms [11]. (In the context of a Bell experiment, where $\{X, A\}$ are space-like separated from $\{Y, B\}$, the conditional independences $A \perp\!\!\!\perp Y|X$, and $B \perp\!\!\!\perp X|Y$ encode the impossibility of sending signals faster than the speed of light.) It is straightforward to check that these conditional independence relations are respected by the P_{ABXY} resulting from Eq. (21). It is well-known that this distribution is nonetheless incompatible with the Bell scenario, for example since it violates the CHSH inequality. Here we prove this incompatibility via the inflation technique, using the inflation of the Bell scenario depicted in Fig. 12.

We begin by noting that $\{A_1B_1X_1Y_1\}$, $\{A_2B_1X_2Y_1\}$, $\{A_1B_2X_1Y_2\}$, $\{A_2B_2X_2Y_2\}$, $\{X_1\}$, $\{X_2\}$, $\{Y_1\}$, and $\{Y_2\}$ are all injectable sets. By Lemma 3, it follows that any causal model that recovers P_{ABXY} inflates to a model that results in marginals

$$P_{A_1B_1X_1Y_1} = P_{A_2B_1X_2Y_1} = P_{A_1B_2X_1Y_2} = P_{A_2B_2X_2Y_2} = P_{ABXY}, \tag{22}$$

$$P_{X_1} = P_{X_2} = P_X, \qquad P_{Y_1} = P_{Y_2} = P_Y. \tag{23}$$

Using the definition of conditional probability, we infer that

$$P_{A_1B_1|X_1Y_1} = P_{A_2B_1|X_2Y_1} = P_{A_1B_2|X_1Y_2} = P_{A_2B_2|X_2Y_2} = P_{AB|XY}. \tag{24}$$

Because $\{X_1\}$, $\{X_2\}$, $\{Y_1\}$, and $\{Y_2\}$ have no common ancestor in the inflated DAG, these variables must be marginally independent in any distribution compatible with the inflated DAG. This applies in particular to the inflation model, so that $P_{X_1X_2Y_1Y_2} = P_{X_1} P_{X_2} P_{Y_1} P_{Y_2}$. Given the assumption that the distributions P_X and P_Y are full support, it follows from Eq. (23) that

$$\text{Sometimes} \quad X_1 = 0, X_2{=}1, Y_1{=}0, Y_2{=}1. \tag{25}$$

---

[8] In the literature on the Bell scenario, these variables are known as "settings". Generally, we may think of endogenous observable variables as settings, coloring them light green in the DAG figures. Settings variables are natural candidates for variables to condition on.

[9] The PR-box is of interest because it represents a manner in which experimental correlations could deviate from the predictions of quantum theory while still being consistent with relativity.

[10] Recall that variables X and Y are conditionally independent given Z if $P_{XY|Z}(xy|z) = P_{X|Z}(x|z) P_{Y|Z}(y|z)$ for all z with $P_Z(z) > 0$. Such a conditional independence is denoted by $X \perp\!\!\!\perp Y \mid Z$.

On the other hand, from Eq. (24) together with the definition of PR-box, Eq. (21), we conclude that

$$\begin{aligned} X_1{=}0, Y_1{=}0 &\implies A_1{=}B_1, \\ X_1{=}0, Y_2{=}1 &\implies A_1{=}B_2, \\ X_2{=}1, Y_1{=}0 &\implies A_2{=}B_1, \\ X_2{=}1, Y_2{=}1 &\implies A_2 \neq B_2. \end{aligned} \tag{26}$$

Combining this with Eq. (25), we obtain

$$\text{Sometimes} \quad A_1{=}B_1, A_1{=}B_2, A_2{=}B_1, A_2 \neq B_2. \tag{27}$$

No values of A_1, A_2, B_1, B_2 can jointly satisfy these conditions—the first three entail perfect correlation between A_2 and B_2, while the fourth entails perfect anti-correlation—so we have reached a contradiction, showing that our original assumption of compatibility between P_{ABXY} and the Bell scenario must have been false.

The structure of this proof parallels that of standard proofs of the incompatibility of the PR-box with the Bell DAG. Standard proofs focus on a set of variables $\{A_0, A_1, B_0, B_1\}$ where A_x is the value of A when $X = x$ and B_y is the value of B when $Y = y$, and note that the distribution $\sum_\lambda P(A_0|\lambda)P(A_1|\lambda)P(B_0|\lambda)P(B_1|\lambda)P(\lambda)$ is a joint distribution over $\{A_0, A_1, B_0, B_1\}$ for which the marginals on pairs $\{A_0, B_0\}$, $\{A_0, B_1\}$, $\{A_1, B_0\}$ and $\{A_1, B_1\}$ are those predicted by the Bell DAG. Finally, the existence of such a joint distribution rules out the possibility of having $A_1{=}B_1, A_1{=}B_2, A_2{=}B_1$ but $A_2 \neq B_2$ and therefore shows that the PR Box correlations are incompatible with the Bell DAG [40, 41]. In light of our use of Eq. (25), our reasoning is really the same argument in disguise.

Appendix F shows that the inflation of Fig. 12, with the number of copies corresponding to the cardinality of X and Y, is enough to witness the incompatibility of any distribution that is indeed incompatible with the Bell scenario.

C. Deriving causal compatibility inequalities

The inflation technique can be used not only to witness the incompatibility of a given distribution with a given causal structure, but also to derive generally applicable necessary conditions that a distribution must satisfy to be compatible with the given causal structure. When these conditions are expressed as inequalities, we will refer to them as *causal compatibility inequalities*. Formally, we have:

Definition 4. *Let G be a causal structure and $S \subseteq \mathsf{ObservedNodes}[G]$. Let I_S denote an inequality that operates on a family of marginal distributions $\{P_{\boldsymbol{U}} : \boldsymbol{U} \in S\}$. Then I_S is a* **causal compatibility inequality for the causal structure** *G whenever it is satisfied by every family of distributions $\{P_{\boldsymbol{U}} : \boldsymbol{U} \in S\}$ that is compatible with G.*

While violation of a causal compatibility inequality witnesses the incompatibility of a distribution with the associated causal structure, the inequality being satisfied does not guarantee that the distribution is compatible with the causal structure. This is the sense in which it merely provides a *necessary* condition for compatibility.

The inflation technique is useful for deriving causal compatibility inequalities because of the following consequence of Lemma 3:

Corollary 5. *Suppose that G' is an inflation of G. Let $S' \subseteq \mathsf{InjectableSets}[G']$ be a family of injectable sets and $S \subseteq \mathsf{ImagesInjectableSets}[G]$ the images of members of S'. Let $I_{S'}$ be a causal compatibility inequality for G' operating on families $\{P_{\boldsymbol{U}'} : \boldsymbol{U}' \in S'\}$. Define an inequality I_S as follows: in the functional form of $I_{S'}$, replace every occurrence of a term $P_{\boldsymbol{U}'}$ by $P_{\boldsymbol{U}}$ for the unique $\boldsymbol{U} \in S$ with $\boldsymbol{U} \sim \boldsymbol{U}'$. Then I_S is a causal compatibility inequality for G operating on families $\{P_{\boldsymbol{U}} : \boldsymbol{U} \in S\}$.*

The proof is as follows. Suppose that the family $\{P_{\boldsymbol{U}} : \boldsymbol{U} \in S\}$ is compatible with G. By Lemma 3, it follows that the family $\{P_{\boldsymbol{U}'} : \boldsymbol{U}' \in S'\}$ where $P_{\boldsymbol{U}'} := P_{\boldsymbol{U}}$ for $\boldsymbol{U}' \sim \boldsymbol{U}$ is compatible with G'. Given that $I_{S'}$ is assumed to be a causal compatibility inequality for G', it follows that $\{P_{\boldsymbol{U}'} : \boldsymbol{U}' \in S'\}$ satisfies $I_{S'}$. But by the definition of I_S, its evaluation on $\{P_{\boldsymbol{U}} : \boldsymbol{U} \in S\}$ is equal to $I_{S'}$ evaluated on $\{P_{\boldsymbol{U}'} : \boldsymbol{U}' \in S'\}$. Since $\{P_{\boldsymbol{U}'} : \boldsymbol{U}' \in S'\}$ satisfies $I_{S'}$, it therefore follows that $\{P_{\boldsymbol{U}} : \boldsymbol{U} \in S\}$ satisfies I_S. Since $\{P_{\boldsymbol{U}} : \boldsymbol{U} \in S\}$ was an arbitrary family compatible with G, it follows that I_S is a causal compatibility inequality for G.

We now present some simple examples of causal compatibility inequalities for the Triangle scenario that one can derive from the inflation technique via Corollary 5.

Some terminology and notation will facilitate the description of these examples. We refer to a pair of nodes which do not share any common ancestor as being **ancestrally independent**. This corresponds to being d-separated by the empty set [1–4]. Given that the conventional notation for X and Y being d-separated by Z in the DAG G is

$X \perp_G Y|Z$, we denote X and Y being ancestrally independent within G as $X \perp_G Y$. Generalizing to sets, $\boldsymbol{U} \perp_G \boldsymbol{V}$ indicates that no node in $\boldsymbol{U}$ shares a common ancestor with any node in $\boldsymbol{V}$ within the DAG G,

$$\boldsymbol{U} \perp_G \boldsymbol{V} \quad \text{iff} \quad \mathsf{An}_G(\boldsymbol{U}) \cap \mathsf{An}_G(\boldsymbol{V}) = \emptyset. \tag{28}$$

Furthermore, the notation $\boldsymbol{U} \perp_G \boldsymbol{V} \perp_G \boldsymbol{W}$ should be understood as indicating that $\boldsymbol{U} \perp_G \boldsymbol{V}$ and $\boldsymbol{V} \perp_G \boldsymbol{W}$ and $\boldsymbol{U} \perp_G \boldsymbol{W}$.

Example 4. **A causal compatibility inequality in terms of *correlators*.**

As in Example 1 of the previous section, consider the cut inflation of the Triangle scenario, depicted in Fig. 8. The injectable sets we make use of here are $\{A_2C_1\}$, $\{B_1C_1\}$, $\{A_2\}$, and $\{B_1\}$.

From Corollary 5, any causal compatibility inequality for the inflated DAG that operates on the marginal distributions of $\{A_2C_1\}$, $\{B_1C_1\}$, $\{A_2\}$, and $\{B_1\}$ will yield a causal compatibility inequality for the original DAG that can evaluated on the marginal distributions for $\{AC\}$, $\{BC\}$, $\{A\}$, and $\{B\}$. We begin, therefore, by identifying a simple example of a causal compatibility inequality for the inflated DAG that is of this sort.

In our example, all of the observed variables are binary. For technical convenience, we assume that these take values in the set $\{-1, +1\}$, rather than taking values in the set $\{0, 1\}$ as was presumed in the last section.

We begin by noting that for *any* distribution on three binary variables $\{A_2B_1C_1\}$, that is, *regardless* of the causal structure in which they are embedded, the marginals on $\{A_2C_1\}$, $\{B_1C_1\}$ and $\{A_2B_1\}$ satisfy the following inequality for expectation values [42–46],

$$\langle A_2C_1\rangle + \langle B_2C_1\rangle - \langle A_2B_1\rangle \leq 1. \tag{29}$$

This is an example of a constraint on pairwise correlators that arises from the presumption that they are consistent with a joint distribution. (The problem of deriving such constraints is the so-called *marginal problem*, discussed in detail in Sec. IV.)

But in the cut inflation of the Triangle scenario (Fig. 8) A_2 and B_1 have no common ancestor and consequently any distribution compatible with this DAG must make A_2 and B_1 marginally independent. In terms of correlators, this can be expressed as

$$A_2 \perp B_1 \implies \langle A_2B_1\rangle = \langle A_2\rangle\langle B_1\rangle. \tag{30}$$

Substituting the latter equality into Eq. (29), we have

$$\langle A_2C_1\rangle + \langle B_2C_1\rangle \leq 1 + \langle A_2\rangle\langle B_1\rangle. \tag{31}$$

This is an example of a simple but nontrivial causal compatibility inequality for the DAG of Fig. 8.

Finally, by Corollary 5, and the fact that the DAG of Fig. 8 is an inflation of the Triangle scenario, we infer that

$$\langle AC\rangle + \langle BC\rangle \leq 1 + \langle A\rangle\langle B\rangle, \tag{32}$$

is a causal compatibility inequality for the Triangle scenario. This inequality expresses the fact that as long as A and B are not completely biased, there is a tradeoff between the strength of AC correlations and the strength of BC correlations.

Given the symmetry of the Triangle scenario under permutations and sign flips of A, B and C, it is clear that the image of inequality Eq. (32) under any such symmetry is also a valid causal compatibility inequality. Together, these inequalities imply monogamy[11] of correlations in the Triangle scenario with binary variables: if any two observed variables with unbiased marginals are perfectly correlated, then they are both uncorrelated with the third.

Example 5. **A causal compatibility inequality in terms of *entropic quantities*.**

One way to derive constraints that are independent of the cardinality of the observed variables is to express these in terms of the mutual information between observed variables rather than in terms of correlators. The inflation technique can also be applied to achieve this. To see how this works in the case of the Triangle scenario, consider again the cut inflation of the Triangle scenario (Fig. 8).

One can follow the same logic as in the preceding example, but starting from a different constraint on marginals. For any distribution on three variables $\{A_2B_1C_1\}$ of arbitrary cardinality (again, regardless of the causal structure in which they are embedded), the marginals on $\{A_2C_1\}$, $\{B_1C_1\}$ and $\{A_2B_1\}$ satisfy the inequality [25, Eq. (29)]

$$I(A_2 : C_1) + I(C_1 : B_1) - I(A_2 : B_1) \leq H(C_1), \tag{33}$$

[11] We are here using the term "monogamy" in the same sort of manner in which it is used in the context of entanglement theory [47].

where $H(X)$ denotes the Shannon entropy of the distribution of X, and $I(X:Y)$ denotes the mutual information between X and Y with respect to the marginal on X and Y.

The fact that A_2 and B_1 have no common ancestor in the inflated DAG implies that in any distribution that is compatible with the inflated DAG, A_2 and B_1 are marginally independent. This is expressed entropically as the vanishing of their mutual information,

$$A_2 \perp B_1 \implies I(A_2 : B_1) = 0. \tag{34}$$

Substituting the latter equality into Eq. (33), we have

$$I(A_2 : C_1) + I(C_1 : B_1) \leq H(C_1). \tag{35}$$

This is another example of a nontrivial causal compatibility inequality for the DAG of Fig. 8.

By Corollary 5, it follows that

$$I(A : C) + I(C : B) \leq H(C), \tag{36}$$

is also a causal compatibility inequality for the Triangle scenario. This inequality was originally derived in [12]. Our rederivation in terms of inflation coincides with the proof found by Henson *et al.* [13].

Example 6. A causal compatibility inequality in terms of *joint probabilities*

Consider the spiral inflation of the Triangle scenario, depicted in Fig. 10, with the injectable sets $\{A_1B_1C_1\}$, $\{A_1B_2\}$, $\{B_1C_2\}$, $\{A_1, C_2\}$, $\{A_2\}$, $\{B_2\}$, and $\{C_2\}$. We here derive a causal compatibility inequality under the assumption that the observed variables are binary, adopting the convention that they take values in $\{0, 1\}$.

We begin by noting that the following is a constraint that holds for any joint distribution of $\{A_1B_1C_1A_2B_2C_2\}$, regardless of the causal structure,

$$P_{A_2B_2C_2}(111) \leq P_{A_1B_1C_1}(000) + P_{A_1B_2C_2}(111) + P_{B_1C_2A_2}(111) + P_{A_2C_1B_2}(111). \tag{37}$$

To prove this claim, it suffices to check that the inequality holds for each of the 2^6 deterministic assignments of values to $\{A_1B_1C_1A_2B_2C_2\}$, from which the general case follows by linearity. A more intuitive proof will be provided in Sec. IV-E.

Next, we note that certain sets of variables have no common ancestors with other sets of variables in the inflated DAG, and we infer the marginal independence of the two sets, expressed now as a factorization of a joint distribution,

$$\begin{aligned} A_1B_2 \perp C_2 &\implies P_{A_1B_2C_2} = P_{A_1B_2}P_{C_2}, \\ B_1C_2 \perp A_2 &\implies P_{B_1C_2A_2} = P_{B_1C_2}P_{A_2}, \\ A_2C_1 \perp B_2 &\implies P_{A_2C_1B_2} = P_{A_2C_1}P_{B_2}, \\ A_2 \perp B_2 \perp C_2 &\implies P_{A_2B_2C_2} = P_{A_2}P_{B_2}P_{C_2}. \end{aligned} \tag{38}$$

Substituting these equations into Eq. (37), we obtain the polynomial inequality

$$P_{A_2}(1)P_{B_2}(1)P_{C_2}(1) \leq P_{A_1B_1C_1}(000) + P_{A_1B_2}(11)P_{C_2}(1) + P_{B_1C_2}(11)P_{A_2}(1) + P_{A_2C_1}(11)P_{B_2}(1). \tag{39}$$

This, therefore, is a causal compatibility inequality for the DAG of Fig. 10. Finally, by Corollary 5, we infer that

$$P_A(1)P_B(1)P_C(1) \leq P_{ABC}(000) + P_{AB}(11)P_C(1) + P_{BC}(11)P_A(1) + P_{AC}(11)P_B(1) \tag{40}$$

is a causal compatibility inequality for the Triangle scenario.

What is distinctive about this inequality is that—through the presence of the term $P_{ABC}(000)$—it takes into account genuine three-way correlations. This inequality is strong enough to demonstrate the incompatibility of the W-type distribution of Eq. (11) with the Triangle scenario: for this distribution, the right-hand side of the inequality vanishes while the left-hand side does not.

Of the known techniques for witnessing the incompatibility of a distribution with a DAG or deriving necessary conditions for compatibility, the most straightforward is to consider the constraints implied by ancestral independences among the observed variables of the DAG. The constraints derived in the last two sections have all made use of this basic technique, but at the level of the inflated DAG rather than the original DAG. The constraints that one thereby infers for the original DAG reflect facts about its causal structure that cannot be expressed in terms of ancestral

independences among its observed variables. The inflation technique manages to expose these facts in the ancestral independences among observed variables of the inflated DAG.

In the rest of this article, we shall continue to rely only on the ancestral independences among observed variables within the inflated DAG to infer compatibility constraints on the original DAG. Nonetheless, it is possible that the inflation technique can also amplify the power of *other* techniques that do not merely consider ancestral independences among the observed variables. We consider some prospects in Sec. V.

IV. SYSTEMATICALLY WITNESSING INCOMPATIBILITY AND DERIVING INEQUALITIES

In the examples from the previous section, the initial inequality—a constraint upon marginals that is independent of the causal structure—involves sets of observed variables that are *not* all injectable. Each of these sets can, however, be partitioned into disjoint subsets each of which *is* injectable whenever the partitioning represents ancestral independence in the inflated DAG. For instance, in the first example from the previous section, the set $\{A_2B_1\}$ is not injectable but it can be partitioned into the singleton sets $\{A_2\}$ and $\{B_1\}$ which are ancestrally independent and each of which is injectable. It is useful to have a name for such sets of observed variables: we call them **pre-injectable**. So for a set of observable nodes $\boldsymbol{U}'$ in the inflated DAG G',

$$\boldsymbol{U}' \in \mathsf{PreInjectableSets}[G'] \quad \text{iff} \quad \exists \{\boldsymbol{U}_i \in \mathsf{InjectableSets}[G']\} \quad \text{s.t.} \quad \boldsymbol{U}' = \bigcup_i \boldsymbol{U}_i \quad \text{and} \quad \forall i \neq j : \boldsymbol{U}_i \perp_{G'} \boldsymbol{U}_j. \tag{41}$$

For example, every injectable set is trivially a pre-injectable set. A pre-injectable set is *maximal* if it is not a proper subset of another pre-injectable set.

Because ancestral independence in the DAG implies statistical independence for any probability distribution compatible with the DAG, it follows that if $\boldsymbol{U}'$ is a pre-injectable set and $\boldsymbol{U}_1, \boldsymbol{U}_2, \ldots, \boldsymbol{U}_n$ are the ancestrally independent components of $\boldsymbol{U}'$, then

$$P_{\boldsymbol{U}'} = P_{\boldsymbol{U}_1} P_{\boldsymbol{U}_2} \cdots P_{\boldsymbol{U}_n} \tag{42}$$

for any distribution compatible with G'. The situation, therefore, is this: for any constraint that one can derive for the marginals on the pre-injectable sets based on the existence of a joint distribution—and hence without reference to the causal structure—one can infer constraints that *do* refer to the causal structure by substituting within these constraints factorizations of the form of Eq. (42).

Thus the pre-injectable sets play a crucial role in linking the original DAG with the inflation DAG: they are precisely those sets of variables whose joint distributions in the inflated model are fully specified by the original causal model on the original DAG: they can be computed using Lemma 3 and Eq. (42). If the resulting family of marginal distributions on pre-injectable sets is not compatible with the existence of a joint distribution, then the original distribution is witnessed as causally incompatible with the original DAG. This is the formal argument underpinning all of the examples in Sec. III-B.

The problem of determining the constraints on marginals that follow from the existence of a joint distribution is known as the *marginal problem*. Thus, we can summarize the situation as follows: an inequality derived from the marginal problem, after applying the factorizations of Eq. (42), becomes a causal compatibility inequality for the inflated DAG. The latter inequality can then be converted into a polynomial causal compatibility inequality for the original DAG using Corollary 5. This section considers the problem of how to implement this procedure systematically.

We limit our attention to deriving causal compatibility inequalities expressed in terms of probabilities[12], as these are generally the most powerful. However, the inflation technique can also be used to derive inequalities expressed in terms of entropies, as our second example from the previous section demonstrated. Indeed, we show in Appendix D that the inflation technique implies the core lemma for deriving non-Shannon-type inequalities.

To obtain a complete solution of the marginal problem, one must determine all the facets of the **marginal polytope**, for which we discuss algorithms in Appendix A. Computing all these facets is computationally costly. It is therefore useful to also consider relaxations of the marginal problem that are less computationally burdensome by deriving valid linear inequalities which may or may not bound the marginal polytope tightly. We describe one such approach based on possibilistic Hardy-type paradoxes and the hypergraph transversal problem. This strategy requires the least computational effort, but is limited in that it only yields inequalities of a very particular form. We describe this approach in Sec. IV-E.

Preliminary to every strategy is the identification of the pre-injectable sets, so we begin with this problem.

[12] Or, for binary variables, equivalently in terms of correlators, as in the first example of Sec. III-C.

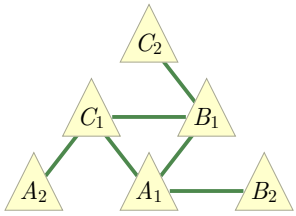

FIG. 13. The injection graph corresponding to the spiral inflation of the Triangle scenario (Fig. 3), wherein a pair of nodes are adjacent iff they are pairwise injectable.

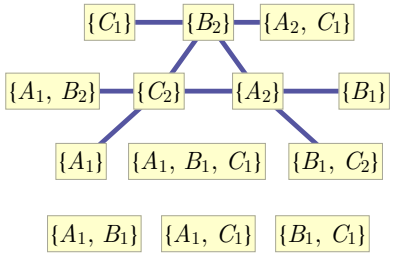

FIG. 14. The pre-injection graph corresponding to the spiral inflation of the Triangle scenario (Fig. 3), wherein a pair of injectable sets are adjacent iff they are ancestrally independent.

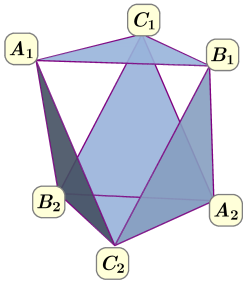

FIG. 15. The simplicial complex of pre-injectable sets for the spiral inflation of the Triangle scenario (Fig. 3). The 5 faces correspond to the maximal pre-injectable sets, namely $\{A_1B_1C_1\}$, $\{A_1B_2C_2\}$, $\{A_2B_1C_2\}$, $\{A_2B_2C_1\}$ and $\{A_2B_2C_2\}$.

A. Identifying the pre-injectable sets

To identify the pre-injectable sets of an inflation DAG, we must first identify the injectable sets. This problem can be reduced to identifying the injectable pairs, because if all of the pairs in a set of nodes are injectable, then so too is the set itself. The latter claim is proven as follows. Let $\varphi : G' \to G$ be the projection map from the inflated DAG G' to the original DAG G, corresponding to removing the copy-indices. Then φ has the characteristic feature that it takes edges to edges: if $A \to B$ in G', then also $\varphi(A) \to \varphi(B)$ in G. Conversely, if $\varphi(A) \to \varphi(B)$ in G then also $A \to B$ in G'; this follows from the assumption that G' is an inflation of G. A set $\boldsymbol{U} \subseteq \mathsf{ObservedNodes}[G']$ is injectable if and only if the restriction of φ to the ancestors of $\boldsymbol{U}$ is an injective map. But now injectivity of a map means precisely that no two different elements of the domain get mapped to the same element of the codomain. So if $\boldsymbol{U}$ is injectable, then so is each of its two-element subsets; conversely, if $\boldsymbol{U}$ is not injectable, then φ maps two nodes among the ancestors of $\boldsymbol{U}$ to the same node, which means that there are two nodes in the ancestry that differ only by copy index. Each of these two nodes must be an ancestor of at least some node in $\boldsymbol{U}$; if one chooses two such descendants, then one gets a two-element subset of $\boldsymbol{U}$ such that φ is not injective on the ancestry of that subset, and therefore this two-element set of observed nodes is not injectable.

To enumerate the injectable sets, it is useful to encode certain features of the inflated DAG in an undirected graph which we call the **injection graph**. The nodes of the injection graph are the observed nodes of the inflated DAG, and a pair of nodes A_i and B_j share an edge if the pair $\{A_iB_j\}$ is injectable. For example, Fig. 13 shows the injection graph of the spiral inflation of the Triangle scenario (Fig. 3). The property noted above states that the injectable sets are precisely the cliques[13] of the injection graph. While for many other other applications only the maximal cliques are of interest, our application of the inflation technique requires knowledge of all nonempty cliques.

Given a list of the injectable sets, the pre-injectable sets can be read off from the **pre-injection graph**. The nodes of the pre-injection graph are taken to be the injectable sets in G', and two nodes share an edge if the associated injectable sets are ancestrally independent. Fig. 14 depicts an example. The pre-injectable sets correspond to the cliques of the pre-injection graph: the union of all the injectable sets that make up the nodes of a clique is a pre-injectable set, while the individual nodes already give us the partition into injectable sets relevant for the factorization relation of Eq. (42). For our purposes, it is sufficient to enumerate the maximal pre-injectable sets, so that one only needs to consider the maximal cliques of the pre-injection graph.

From Figs. 13 and 14, we easily infer the injectable sets and the maximal pre-injectable sets, as well as the partition of the maximal pre-injectable sets into ancestrally independent subsets, for the spiral inflation of the Triangle scenario

[13] A *clique* is a set of nodes in an undirected graph any two of which share an edge.

(Fig. 3)to be:

$$\underbrace{\begin{array}{c}\{A_1\},\ \{B_1\},\ \{C_1\},\\ \{A_2\},\ \{B_2\},\ \{C_2\},\\ \{A_1B_1\},\ \{A_1C_1\},\ \{B_1C_1\},\\ \{A_1B_2\}.\{A_2C_1\},\ \{B_1C_2\},\\ \{A_1B_1C_1\}\end{array}}_{\text{injectable sets}} \qquad \underbrace{\begin{array}{c}\{A_1B_1C_1\}\\ \{A_1B_2C_2\}\\ \{B_1C_2A_2\}\\ \{C_1A_2B_2\}\\ \{A_2B_2C_2\}\end{array}}_{\begin{array}{c}\text{maximal}\\ \text{pre-injectable sets}\end{array}} \qquad \underbrace{\begin{array}{c}\{A_1B_2\}\perp\{C_2\}\\ \{B_1C_2\}\perp\{A_2\}\\ \{C_1A_2\}\perp\{B_2\}\\ \{A_2\}\perp\{B_2\}\perp\{C_2\}\end{array}}_{\begin{array}{c}\text{relevant}\\ \text{ancestral independences}\end{array}} \tag{43}$$

Using the ancestral independence relations, the marginal distributions for the maximal pre-injectable sets factorize in the manner described by the right-hand side of Eq. (38).

Having identified the pre-injectable sets together with the factorization relations implied by ancestral independences, we now discuss how to obtain constraints on the marginal distributions over the pre-injectable sets.

B. The marginal problem

For a given family of marginal distributions, each defined on a subset of the variables, determining whether there exists a joint probability distribution over the full set of variables from which all of these can be obtained as marginal distributions is known as the *marginal problem*. For some of its history and for further references, see [25]; for a more modern account using the language of presheaves, see [48].

To specify such a problem, one must specify the full set of variables to be considered, denoted $\boldsymbol{X}$, together with a family of subsets of $\boldsymbol{X}$, denoted $(\boldsymbol{U}_1, \ldots, \boldsymbol{U}_n)$ and called **contexts**. A family of contexts can be visualized through the simplicial complex that they generate, as the example in Fig. 15 illustrates. Every joint distribution $P_{\boldsymbol{X}}$ defines a family of marginal distributions, $(P_{\boldsymbol{U}_1}, \ldots, P_{\boldsymbol{U}_n})$ through marginalization, $P_{\boldsymbol{U}_i} := \sum_{\boldsymbol{X}\setminus\boldsymbol{U}_i} P_{\boldsymbol{X}}$. A *marginal problem* concerns the converse inference. A family of distributions $(P_{\boldsymbol{U}_1}, \ldots, P_{\boldsymbol{U}_n})$ is given, and one wants to find conditions for when a joint distribution $\hat{P}_{\boldsymbol{X}}$ exists which reproduces the given marginals, $P_{\boldsymbol{U}_i} = \sum_{\boldsymbol{X}\setminus\boldsymbol{U}_i} \hat{P}_{\boldsymbol{X}}$ for all i.

There is a simple necessary condition: in order for $\hat{P}_{\boldsymbol{X}}$ to exist, the marginals clearly must be consistent, in the sense that marginalizing $P_{\boldsymbol{U}_i}$ to the variables in $\boldsymbol{U}_i \cap \boldsymbol{U}_j$ results in the same distribution as marginalizing $P_{\boldsymbol{U}_j}$ to those variables. In many cases this is not sufficient; indeed, we have already seen examples of additional constraints, namely, the inequalities (29), (33) and (37) from Sec. III-C[14]. So what are the necessary and sufficient conditions?

To answer this question, it helps to realize two things:

- The set of possibilities for the distribution $P_{\boldsymbol{X}}$ is the convex hull of the deterministic assignments of values to $\boldsymbol{X}$ (the point distributions), and
- The map $P_{\boldsymbol{X}} \to (P_{\boldsymbol{U}_1}, \ldots, P_{\boldsymbol{U}_n})$, describing marginalization to each of the contexts in $(\boldsymbol{U}_1, \ldots, \boldsymbol{U}_n)$, is linear.

Hence the image of the set of possibilities for the distribution $P_{\boldsymbol{X}}$ under the map $P_{\boldsymbol{X}} \to (P_{\boldsymbol{U}_1}, \ldots, P_{\boldsymbol{U}_n})$ is exactly the convex hull of the deterministic assignments of values to $(\boldsymbol{U}_1, \ldots, \boldsymbol{U}_n)$ (more precisely, the deterministic assignments that are consistent where these contexts overlap). Since there are only finitely many such deterministic assignments, this convex hull is a polytope; it is called the **marginal polytope** [50]. Together with the above equations on coinciding submarginals, the facet inequalities of the marginal polytope form necessary and sufficient conditions for the marginal problem to have a solution.

As every facet enumeration problem, this can also be phrased as a problem of **linear quantifier elimination**. We illustrate this with the example of the marginal problem where $\boldsymbol{X} := \{A_1, A_2, B_1, B_2, C_1, C_2\}$ and the contexts are the maximal pre-injectable sets in Eq. (43). Besides normalization of probability, the only constraint on the probabilities making up the joint distribution is nonnegativity,

$$\forall a_1 a_2 b_1 b_2 c_1 c_2 :\ P_{A_1A_2B_1B_2C_1C_2}(a_1a_2b_1b_2c_1c_2) \geq 0. \tag{44}$$

---

[14] Depending on how the contexts intersect with one another, this *may* be sufficient. A precise characterization for when this occurs has been found by Vorob'ev [49].

We require the joint distribution to reproduce the marginal distribution on each context via

$$\begin{aligned}
\forall a_1b_1c_1:\ P_{A_1B_1C_1}(a_1b_1c_1) &= \sum\nolimits_{a_2b_2b_2} P_{A_1A_2B_1B_2C_1C_2}(a_1a_2b_1b_2c_1c_2),\\
\forall a_1b_2c_2:\ P_{A_1B_2C_2}(a_1b_2c_2) &= \sum\nolimits_{a_2b_1c_1} P_{A_1A_2B_1B_2C_1C_2}(a_1a_2b_1b_2c_1c_2),\\
\forall a_2b_1c_2:\ P_{A_2B_1C_2}(a_2b_1c_2) &= \sum\nolimits_{a_1b_2c_1} P_{A_1A_2B_1B_2C_1C_2}(a_1a_2b_1b_2c_1c_2),\\
\forall a_2b_2c_1:\ P_{A_2B_2C_1}(a_2b_2c_1) &= \sum\nolimits_{a_1b_1c_2} P_{A_1A_2B_1B_2C_1C_2}(a_1a_2b_1b_2c_1c_2),\\
\forall a_2b_2c_2:\ P_{A_2B_2C_2}(a_2b_2c_2) &= \sum\nolimits_{a_1b_1c_1} P_{A_1A_2B_1B_2C_1C_2}(a_1a_2b_1b_2c_1c_2).
\end{aligned} \tag{45}$$

If each variable is binary, then we have 64 inequalities and 40 equations, although the latter are not all independent.

The marginal problem is a linear system of equations and inequalities relating the unknown joint probabilities to the accessible marginal probabilities. The problem of quantifier elimination consists in finding an equivalent system of equations and inequalities that is satisfied if and only if the original system has a solution for the unknown probabilities. This requires eliminating 64 unknowns $P_{A_1A_2B_1B_2C_1C_2}(a_1a_2b_1b_2c_1c_2)$ for each of the 64 choices of the values $a_1, \ldots, c_2$. The resulting new system consists of the coinciding-submarginals equations together with the facet inequalities of the marginal polytope.

It is helpful to formalize the marginal problem in terms of a **marginal description matrix $\boldsymbol{M}$**, a **marginal distribution vector $\boldsymbol{b}$**, and some unknown **joint distribution vector $\boldsymbol{x}$**. The marginal problem can the be stated as

$$\exists_{\boldsymbol{x}\geq\boldsymbol{0}} \text{ s.t. } \boldsymbol{M}.\boldsymbol{x} = \boldsymbol{b} \tag{46}$$

where in the example we have been discussing $\boldsymbol{M}$ would be a 48×64 matrix, such that $\boldsymbol{M}.\boldsymbol{x} = \boldsymbol{b}$ represents 48 equations and $\boldsymbol{x} \geq \boldsymbol{0}$ represents 64 inequalities. Note that the marginal description matrix $\boldsymbol{M}$ has only zeroes and ones as its constituent elements.

Linear quantifier elimination is already used in causal inference for deriving entropic causal compatibility inequalities [16, 24]. In that task, however, the unknowns being eliminated are entropies on sets of variables of which one or more is latent. By contrast, the unknowns being eliminated above are all probabilities on sets of variables all of which are observed—but on the inflated DAG rather than the original DAG. Appendix F will partly elucidate the relation.

The marginal problem is a standard facet enumeration problem, in that the vertices of the polytope are given. The derivation of entropic inequalities, by contrast, is a priori only a linear quantifier elimination task, and more difficult to cast as a facet enumeration problem with given vertices, since the vertices (extremal rays) of the Shannon cone elude a simple description. As such, while facet enumeration tools are useful for deriving polynomial inequalities via the inflation technique, they are not directly available for the derivation of entropic inequalities; see Appendix A for further details.

C. Witnessing incompatibility by non-sastisfiability of the marginal problem

Given a particular distribution on observed nodes of the original DAG, one can use the inflation technique to probe causal compatibility as follows. Using Lemma 3 along with the factorization conditions implied by ancestral independences among the variables in the maximal pre-injectable sets, one can infer the distributions on the maximal pre-injectable sets that are implied by the given distribution on the images of these in the original DAG; this was the first step in each example in Sec. III-B. This amounts to having known numerical values for the marginal distribution vector $\boldsymbol{b}$ in Eq. (46), which we denote $\boldsymbol{b}_{\text{numeric}}$. A single linear program can then assess whether the marginal problem equalities, i.e., the matrix equality of Eq. (46),can be solved using nonnegative values for the unknown joint probabilities, $\boldsymbol{x} \geq \boldsymbol{0}$, or not. If the marginal problem cannot be satisfied, then the original distribution is witnessed as incompatible with the original DAG.

As this satisfiability problem is a linear program, testing specific distributions for causal compatibility for a given inflation DAG is computationally inexpensive. For instance, using the rather complex web inflation of the Triangle scenario, depicted in Fig. 2, our numerical computations have reproduced the result of [12, Theorem 2.16], that a certain distribution considered therein is incompatible with the Triangle scenario.[15].

[15] This distribution *is*, however, quantum-compatible with the Triangle scenario. It was constructed from a distribution that is quantum-compatible but classically-incompatible with the Bell scenario.

When $\boldsymbol{M}.\boldsymbol{x} = \boldsymbol{b}_{\text{numeric}}$ has no positive solution $\boldsymbol{x}$ then the system is considered **primal infeasible**. Many linear programming tools are capable of returning a **Farkas infeasibility certificate** [51] whenever a linear system is primal infeasible[16]. The infeasibility certificate is a vector $\boldsymbol{y}$ of the same length as $\boldsymbol{b}_{\text{numeric}}$ which can be used to generate the (scalar) marginal-consistency inequality $\boldsymbol{y}.\boldsymbol{b} \geq 0$ which is violated for $\boldsymbol{b} \to \boldsymbol{b}_{\text{numeric}}$. One can readily verify that the infeasibility certificate $\boldsymbol{y}$ maps the marginal description matrix $\boldsymbol{M}$ to some nonnegtive vector; that is to say $\boldsymbol{y}.\boldsymbol{M} \geq \boldsymbol{0}$, so that

$$\exists_{\boldsymbol{x} \geq \boldsymbol{0}} \text{ s.t. } \boldsymbol{y}.\boldsymbol{M}.\boldsymbol{x} = \boldsymbol{y}.\boldsymbol{b} \quad \implies \quad \boldsymbol{y}.\boldsymbol{b} \geq 0 \tag{47}$$

D. Causal compatibility inequalities via a complete solution of the marginal problem

For deriving causal compatibility inequalities systematically, one chooses an inflation DAG and identifies the maximal pre-injectable sets, as described above. Then ones solves the marginal problem via facet enumeration[17] of the marginal polytope, where the contexts are the maximal pre-injectable sets. This results in linear inequalities at the level of the inflation DAG. By substituting into these inequalities the factorization conditions implied by ancestral independences per Eq. (42), one obtains causal compatibility inequalities for the inflated DAG. Finally, these can be converted into causal compatibility inequalities for the original DAG using Corollary 5.

As an example, we present all of the causal compatibility inequalities that one can derive for the Triangle scenario with binary observed variables using the spiral inflation of the Triangle scneario (Fig. 3). The contexts for the marginal problem are the maximal pre-injectable sets of Eq. (43) and Fig. 15. We solve this marginal problem using facet enumeration. It turns out that the marginal polytope has 64 symmetry classes of facets, where the symmetry transformations are given by permutations of the observed variables, by flipping the value of one variable, and by composites of these. Applying the factorization of probabilities according to ancestral independences per Eq. (43) and converting into inequalities for the original DAG using Corollary 5 results in 64 polynomial inequalities up to symmetry. However, there is no guarantee that each one of these inequalities is nontrivial at the level of the original DAG, where nontriviality of an inequality means that it is violated by at least one distribution. Numerically, we find that only 37 of these inequalities are indeed nontrivial. We present all 37 symmetry classes of causal compatibility inequalities here in correlator form[18] (A star next to the index of an inequality indicates that the inequality can also be derived by considering the possibilisitc marginal problem per Sec. IV-E in lieu of solving the standard (probabilistic)

[16] Farkas infeasibility certificates are available, for example, in *Mosek*, *Gurobi*, and *CPLEX*, as well as by accessing dual variables in *cvxr*/*cvxopt*.
[17] In Appendix A, we provide an overview of techniques for facet enumeration.
[18] A machine-readable version of this list of inequalities may be found in Appendix E.

marginal problem described above.):

$$
\begin{aligned}
&(\#1^*): && 0 \leq 1 + \langle B\rangle\langle C\rangle + \langle AB\rangle + \langle AC\rangle \\
&(\#2): && 0 \leq 2 + \langle A\rangle\langle B\rangle\langle C\rangle - \langle C\rangle\langle AB\rangle - 2\langle AC\rangle \\
&(\#3^*): && 0 \leq 3 + \langle A\rangle - \langle B\rangle + \langle C\rangle + \langle B\rangle\langle C\rangle + \langle A\rangle\langle B\rangle\langle C\rangle + \langle AB\rangle - \langle C\rangle\langle AB\rangle + 3\langle AC\rangle - \langle B\rangle\langle AC\rangle \\
&(\#4^*): && 0 \leq 3 + \langle A\rangle - \langle B\rangle + \langle C\rangle + \langle B\rangle\langle C\rangle - \langle A\rangle\langle B\rangle\langle C\rangle + \langle AB\rangle + \langle C\rangle\langle AB\rangle + 3\langle AC\rangle - \langle B\rangle\langle AC\rangle \\
&(\#5): && 0 \leq 3 + \langle B\rangle - \langle A\rangle\langle B\rangle + \langle A\rangle\langle C\rangle + \langle A\rangle\langle B\rangle\langle C\rangle + \langle AB\rangle + \langle C\rangle\langle AB\rangle - \langle B\rangle\langle AC\rangle - 2\langle BC\rangle \\
&(\#6): && 0 \leq 3 + \langle B\rangle + \langle A\rangle\langle C\rangle + \langle A\rangle\langle B\rangle\langle C\rangle - \langle C\rangle\langle AB\rangle - 2\langle AC\rangle - \langle B\rangle\langle AC\rangle - 2\langle BC\rangle \\
&(\#7): && 0 \leq 3 + \langle B\rangle + \langle A\rangle\langle B\rangle - \langle A\rangle\langle C\rangle - \langle A\rangle\langle B\rangle\langle C\rangle + \langle AB\rangle + \langle C\rangle\langle AB\rangle + \langle B\rangle\langle AC\rangle - 2\langle BC\rangle \\
&(\#8^*): && 0 \leq 3 + \langle A\rangle + \langle B\rangle + \langle A\rangle\langle B\rangle + \langle C\rangle + \langle A\rangle\langle C\rangle + \langle B\rangle\langle C\rangle - \langle A\rangle\langle B\rangle\langle C\rangle + 2\langle AB\rangle + \langle C\rangle\langle AB\rangle + 2\langle AC\rangle + \langle B\rangle\langle AC\rangle + 2\langle BC\rangle + \langle A\rangle\langle BC\rangle - \langle ABC\rangle \\
&(\#9^*): && 0 \leq 3 + \langle A\rangle + \langle B\rangle - \langle A\rangle\langle B\rangle + \langle C\rangle + \langle A\rangle\langle C\rangle + \langle B\rangle\langle C\rangle - \langle A\rangle\langle B\rangle\langle C\rangle + \langle C\rangle\langle AB\rangle + 2\langle AC\rangle + \langle B\rangle\langle AC\rangle - 2\langle BC\rangle - \langle A\rangle\langle BC\rangle + \langle ABC\rangle \\
&(\#10^*): && 0 \leq 4 + 2\langle A\rangle\langle B\rangle + 2\langle C\rangle + 2\langle B\rangle\langle C\rangle - 2\langle AB\rangle + \langle C\rangle\langle AB\rangle - 2\langle AC\rangle + \langle B\rangle\langle AC\rangle + \langle A\rangle\langle BC\rangle - \langle ABC\rangle \\
&(\#11^*): && 0 \leq 4 - 2\langle B\rangle + \langle B\rangle\langle C\rangle + \langle A\rangle\langle B\rangle\langle C\rangle - 2\langle AB\rangle + \langle C\rangle\langle AB\rangle - \langle B\rangle\langle AC\rangle - 3\langle BC\rangle + \langle ABC\rangle \\
&(\#12^*): && 0 \leq 4 - 2\langle B\rangle + 2\langle A\rangle\langle C\rangle + \langle B\rangle\langle C\rangle - \langle A\rangle\langle B\rangle\langle C\rangle - 2\langle AB\rangle + \langle C\rangle\langle AB\rangle - 2\langle AC\rangle + \langle B\rangle\langle AC\rangle - 3\langle BC\rangle + \langle ABC\rangle \\
&(\#13^*): && 0 \leq 4 - 2\langle A\rangle\langle B\rangle - 2\langle A\rangle\langle C\rangle - \langle B\rangle\langle C\rangle - \langle A\rangle\langle B\rangle\langle C\rangle + 2\langle AB\rangle - \langle C\rangle\langle AB\rangle - 2\langle AC\rangle + \langle B\rangle\langle AC\rangle + \langle BC\rangle + \langle ABC\rangle \\
&(\#14^*): && 0 \leq 4 - 2\langle A\rangle\langle B\rangle + 2\langle A\rangle\langle C\rangle - \langle B\rangle\langle C\rangle + \langle A\rangle\langle B\rangle\langle C\rangle + 2\langle AB\rangle + \langle C\rangle\langle AB\rangle - 2\langle AC\rangle + \langle B\rangle\langle AC\rangle + \langle BC\rangle + \langle ABC\rangle \\
&(\#15^*): && 0 \leq 4 + 2\langle A\rangle\langle C\rangle + \langle B\rangle\langle C\rangle + \langle A\rangle\langle B\rangle\langle C\rangle - \langle C\rangle\langle AB\rangle - 2\langle AC\rangle - \langle B\rangle\langle AC\rangle + 3\langle BC\rangle + \langle ABC\rangle \\
&(\#16^*): && 0 \leq 4 - 2\langle B\rangle + 2\langle A\rangle\langle C\rangle - 2\langle AB\rangle + \langle C\rangle\langle AB\rangle - 2\langle AC\rangle + \langle B\rangle\langle AC\rangle - 2\langle BC\rangle - \langle A\rangle\langle BC\rangle + \langle ABC\rangle \\
&(\#17^*): && 0 \leq 4 + 2\langle A\rangle\langle B\rangle + 2\langle A\rangle\langle C\rangle + 2\langle B\rangle\langle C\rangle - 2\langle AB\rangle + \langle C\rangle\langle AB\rangle - 2\langle AC\rangle + \langle B\rangle\langle AC\rangle - 2\langle BC\rangle + \langle A\rangle\langle BC\rangle + \langle ABC\rangle \\
&(\#18): && 0 \leq 5 + \langle A\rangle + \langle B\rangle - 2\langle A\rangle\langle B\rangle + \langle C\rangle + \langle B\rangle\langle C\rangle + \langle A\rangle\langle B\rangle\langle C\rangle + 3\langle AB\rangle + \langle C\rangle\langle AB\rangle + \langle AC\rangle - \langle B\rangle\langle AC\rangle - 4\langle BC\rangle \\
&(\#19^*): && 0 \leq 5 + \langle A\rangle + \langle B\rangle + 2\langle A\rangle\langle B\rangle + \langle C\rangle - 2\langle A\rangle\langle C\rangle + \langle B\rangle\langle C\rangle - \langle A\rangle\langle B\rangle\langle C\rangle + 3\langle AB\rangle + \langle C\rangle\langle AB\rangle - \langle AC\rangle + \langle B\rangle\langle AC\rangle - 4\langle BC\rangle \\
&(\#20^*): && 0 \leq 5 + \langle A\rangle - \langle B\rangle - 2\langle A\rangle\langle B\rangle + \langle C\rangle - \langle A\rangle\langle C\rangle + \langle B\rangle\langle C\rangle + \langle AB\rangle + \langle C\rangle\langle AB\rangle + 2\langle AC\rangle - 2\langle B\rangle\langle AC\rangle - 2\langle BC\rangle - 2\langle A\rangle\langle BC\rangle - 2\langle ABC\rangle \\
&(\#21^*): && 0 \leq 5 + \langle A\rangle + \langle B\rangle + \langle C\rangle - \langle A\rangle\langle C\rangle - \langle B\rangle\langle C\rangle - 2\langle A\rangle\langle B\rangle\langle C\rangle + \langle AB\rangle + 2\langle C\rangle\langle AB\rangle + 2\langle AC\rangle + \langle B\rangle\langle AC\rangle - 2\langle BC\rangle + \langle A\rangle\langle BC\rangle - \langle ABC\rangle \\
&(\#22^*): && 0 \leq 5 - \langle A\rangle + \langle B\rangle - 2\langle A\rangle\langle B\rangle + \langle C\rangle - 2\langle A\rangle\langle C\rangle + 2\langle B\rangle\langle C\rangle + \langle AB\rangle - 2\langle C\rangle\langle AB\rangle + \langle AC\rangle - 2\langle B\rangle\langle AC\rangle - \langle BC\rangle - 2\langle A\rangle\langle BC\rangle + \langle ABC\rangle \\
&(\#23^*): && 0 \leq 5 + \langle A\rangle + \langle B\rangle - \langle A\rangle\langle B\rangle + \langle C\rangle + 2\langle B\rangle\langle C\rangle + \langle A\rangle\langle B\rangle\langle C\rangle + 2\langle AB\rangle - \langle C\rangle\langle AB\rangle + \langle AC\rangle - 2\langle B\rangle\langle AC\rangle - \langle BC\rangle - 2\langle A\rangle\langle BC\rangle + \langle ABC\rangle \\
&(\#24^*): && 0 \leq 5 + \langle A\rangle + \langle B\rangle - 2\langle A\rangle\langle B\rangle + \langle C\rangle - \langle A\rangle\langle C\rangle - \langle B\rangle\langle C\rangle - 2\langle A\rangle\langle B\rangle\langle C\rangle - \langle AB\rangle + 2\langle C\rangle\langle AB\rangle + 2\langle AC\rangle + \langle B\rangle\langle AC\rangle + 2\langle BC\rangle - \langle A\rangle\langle BC\rangle + \langle ABC\rangle \\
&(\#25): && 0 \leq 6 + 2\langle A\rangle\langle B\rangle + \langle A\rangle\langle C\rangle + 2\langle B\rangle\langle C\rangle + \langle A\rangle\langle B\rangle\langle C\rangle - 4\langle AB\rangle - 2\langle C\rangle\langle AB\rangle - 3\langle AC\rangle - \langle B\rangle\langle AC\rangle - 2\langle A\rangle\langle BC\rangle \\
&(\#26): && 0 \leq 6 - 2\langle A\rangle + \langle A\rangle\langle B\rangle + 2\langle C\rangle + \langle A\rangle\langle C\rangle + 2\langle A\rangle\langle B\rangle\langle C\rangle - 5\langle AB\rangle - \langle C\rangle\langle AB\rangle - 3\langle AC\rangle + \langle B\rangle\langle AC\rangle - 2\langle A\rangle\langle BC\rangle \\
&(\#27): && 0 \leq 6 + 2\langle A\rangle\langle B\rangle + 2\langle C\rangle + \langle A\rangle\langle C\rangle + \langle A\rangle\langle B\rangle\langle C\rangle - 4\langle AB\rangle - 2\langle C\rangle\langle AB\rangle + 3\langle AC\rangle + \langle B\rangle\langle AC\rangle - 2\langle A\rangle\langle BC\rangle \\
&(\#28): && 0 \leq 6 + \langle A\rangle\langle B\rangle + \langle A\rangle\langle C\rangle - 4\langle B\rangle\langle C\rangle - 2\langle A\rangle\langle B\rangle\langle C\rangle + \langle AB\rangle + \langle C\rangle\langle AB\rangle - 3\langle AC\rangle - \langle B\rangle\langle AC\rangle + 2\langle BC\rangle - 2\langle A\rangle\langle BC\rangle \\
&(\#29): && 0 \leq 6 + 2\langle B\rangle + \langle A\rangle\langle B\rangle - 2\langle A\rangle\langle C\rangle + \langle B\rangle\langle C\rangle - 2\langle A\rangle\langle B\rangle\langle C\rangle + 3\langle AB\rangle + \langle C\rangle\langle AB\rangle + 2\langle B\rangle\langle AC\rangle - 5\langle BC\rangle + \langle A\rangle\langle BC\rangle \\
&(\#30): && 0 \leq 6 + 2\langle B\rangle - 2\langle A\rangle\langle B\rangle + 4\langle A\rangle\langle C\rangle - \langle B\rangle\langle C\rangle + \langle A\rangle\langle B\rangle\langle C\rangle + 2\langle AB\rangle + 2\langle C\rangle\langle AB\rangle - 2\langle AC\rangle + 2\langle B\rangle\langle AC\rangle + \langle BC\rangle + \langle A\rangle\langle BC\rangle \\
&(\#31): && 0 \leq 6 + \langle A\rangle\langle C\rangle + 4\langle B\rangle\langle C\rangle + \langle A\rangle\langle B\rangle\langle C\rangle - 2\langle AB\rangle - 2\langle C\rangle\langle AB\rangle - 3\langle AC\rangle - \langle B\rangle\langle AC\rangle - 2\langle BC\rangle - 2\langle ABC\rangle \\
&(\#32): && 0 \leq 7 + \langle A\rangle + \langle B\rangle + \langle A\rangle\langle B\rangle + \langle C\rangle - 2\langle A\rangle\langle C\rangle + 2\langle B\rangle\langle C\rangle - \langle A\rangle\langle B\rangle\langle C\rangle + 2\langle AB\rangle + 3\langle C\rangle\langle AB\rangle + \langle AC\rangle + 2\langle B\rangle\langle AC\rangle - 3\langle BC\rangle - 2\langle A\rangle\langle BC\rangle + 3\langle ABC\rangle \\
&(\#33): && 0 \leq 8 + 2\langle A\rangle\langle B\rangle + 4\langle A\rangle\langle C\rangle - 2\langle B\rangle\langle C\rangle + 2\langle A\rangle\langle B\rangle\langle C\rangle - 2\langle AB\rangle - \langle C\rangle\langle AB\rangle - 4\langle AC\rangle + \langle B\rangle\langle AC\rangle - 2\langle BC\rangle - 3\langle A\rangle\langle BC\rangle - 3\langle ABC\rangle \\
&(\#34): && 0 \leq 8 + 2\langle A\rangle - 2\langle C\rangle - \langle A\rangle\langle C\rangle + 2\langle B\rangle\langle C\rangle + 3\langle A\rangle\langle B\rangle\langle C\rangle - 6\langle AB\rangle + \langle C\rangle\langle AB\rangle + \langle AC\rangle + 2\langle B\rangle\langle AC\rangle - 3\langle A\rangle\langle BC\rangle + \langle ABC\rangle \\
&(\#35): && 0 \leq 8 + 2\langle A\rangle + \langle A\rangle\langle C\rangle + 2\langle B\rangle\langle C\rangle + 3\langle A\rangle\langle B\rangle\langle C\rangle + 6\langle AB\rangle - \langle C\rangle\langle AB\rangle + \langle AC\rangle - 2\langle B\rangle\langle AC\rangle - 2\langle BC\rangle - 3\langle A\rangle\langle BC\rangle + \langle ABC\rangle \\
&(\#36): && 0 \leq 8 - 2\langle B\rangle + 2\langle A\rangle\langle B\rangle - 2\langle C\rangle - \langle B\rangle\langle C\rangle - 3\langle A\rangle\langle B\rangle\langle C\rangle + 3\langle C\rangle\langle AB\rangle - 6\langle AC\rangle + \langle B\rangle\langle AC\rangle + \langle BC\rangle - 2\langle A\rangle\langle BC\rangle + \langle ABC\rangle \\
&(\#37): && 0 \leq 8 + 2\langle B\rangle + \langle A\rangle\langle B\rangle - 2\langle A\rangle\langle C\rangle - 3\langle A\rangle\langle B\rangle\langle C\rangle + \langle AB\rangle + 2\langle C\rangle\langle AB\rangle + 2\langle AC\rangle + 3\langle B\rangle\langle AC\rangle - 6\langle BC\rangle - \langle A\rangle\langle BC\rangle + \langle ABC\rangle
\end{aligned}
$$

It is likely that these 37 symmetry classes of causal compatibility inequalities are not a minimal generating set, where a minimal generating set is defined to be one such that, for every inequality, there is a distribution that violates it while satisfying all of the others.

E. Causal compatibility inequalities via Hardy-type inferences from logical tautologies

Enumerating all the facets of the marginal polytope is computationally feasible only for relatively small examples. But our method still applies when only some inequalities that bound the marginal polytope are known, and we now present a general approach for deriving such inequalities very quickly.

In the literature on Bell inequalities, it has been noticed that incompatibility with the Bell DAG can sometimes be witnessed by merely looking at which joint outcomes have zero probability and which ones have nonzero probability. In other words, instead of considering the *probability* of an outcome, the inconsistency of some marginal distributions can be evident from considering only the *possibility* or *impossibility* of each outcome. This insight is originally due to Hardy [32], and versions of Bell's theorem that are based on the violation of such **possibilistic constraints** are known as **Hardy-type paradoxes** [40, 52–55]; a partial classification of these can be found in [33].

In this approach, the constraints follow from a consideration of *logical relations* that can hold among deterministic assignments to the observed variables. Such logical constraints can also be leveraged to derive probabilistic constraints instead of possibilistic ones, as shown in [43, 56]. This results in a partial solution to any given (probabilistic) marginal problem. Essentially, we solve a possibilistic marginal problem [33], then upgrade the possibilistic inequalities into probabilistic inequalities, resulting in a set of probabilistic inequalities whose cumulative satisfaction is a necessary but insufficient condition for satisfying the corresponding probabilistic marginal problem. We now demonstrate how to systematically derive all inequalities of this type.

We have already provided a simple example of a Hardy-type argument in Sec. III-C, in the logic used to demonstrate that the marginal distributions of Eqs. (15-17) are incompatible with the DAG depicted in Fig. 10. For our present purposes, it is useful to recast the argument of Sec. III-C into a new but manifestly equivalent form.

First, for the distribution in question, we have

$$\begin{aligned} A_2{=}1 &\implies C_1{=}0 \\ B_2{=}1 &\implies A_1{=}0 \\ C_2{=}1 &\implies B_1{=}0 \\ \text{Never} \quad A_1{=}0 \text{ and } B_1{=}0 &\text{ and } C_1{=}0. \end{aligned} \tag{48}$$

From the last constraint one infers that at least one of A_1, B_1 and C_1 must be 1, which from the three other constraints implies that at least one of A_2, B_2 and C_2 must be 0, so that it is not the case that all of A_2, B_2 and C_2 are 1. Thus Eq. (48) implies

$$\text{Never} \quad A_2{=}1 \text{ and } B_2{=}1 \text{ and } C_2{=}1. \tag{49}$$

However, the DAG of Fig. 10 is such that A_2,B_2, and C_2 have no common ancestor and consequently these variables are marginally independent in any distribution consistent with this DAG. Combining this with the fact that the marginal distribution for each of these three variables has full support implies that A_2,B_2, and C_2 sometimes all take the value 1, which contradicts Eq. (49). What is nice about this form of the reasoning is that the appeal to the causal structure occurs only in the very last step.

We are here interested in recasting the argument in such a way that the appeal to *both* the causal structure *and* the form of the marginal distributions occurs only in the very last step. This is done as follows. The first step of the argument is to note that the following proposition is a logical tautology for binary variables (here, $\wedge$, $\vee$ and $\neg$ denote conjunction, disjunction and negation respectively):

$$\begin{aligned} &\neg[A_2{=}1 \wedge C_1{=}1] \bigwedge \neg[B_2{=}1 \wedge A_1{=}1] \bigwedge \neg[C_2{=}1 \wedge B_1{=}1] \bigwedge \neg[A_1{=}0 \wedge B_1{=}0 \wedge C_1{=}0] \\ &\qquad \implies \neg[A_2{=}1 \wedge B_2{=}1 \wedge C_2{=}1]. \end{aligned} \tag{50}$$

The second and final step of the argument notes that the given distribution and the given causal structure imply that the antecedent is true while the consequent is false, so that the distribution and causal structure together imply a contradiction.

In our recasting of the Hardy-type argument, the first step—identifying a logical tautology among valuations of certain subsets of the variables— can be understood as a constraint on marginal *deterministic assignments*, and it is a constraint that follows from logic alone. It is useful to think of this first step as the logical counterpart of a constraint on marginals.

We illustrate this last claim with the example just discussed. It can be cast as a marginal scenario where the contexts are $\{A_2B_2C_2\}$, $\{A_2C_1\}$, $\{B_2A_1\}$, $\{C_2B_1\}$, and $\{A_1B_1C_1\}$. The logical tautology (50) is then a constraint on marginal determinstic assignments for this marginal scenario. To see how to obtain a constraint on marginal *distributions*, we start by rewriting Eq. (50) in its contrapositive form ("and" now implicit in the brackets)

$$[\mathbf{A_2{=}1}, \mathbf{B_2{=}1}, \mathbf{C_2{=}1}] \implies [\mathbf{A_2{=}1}, C_1{=}1] \vee [\mathbf{B_2{=}1}, A_1{=}1] \vee [\mathbf{C_2{=}1}, B_1{=}1] \vee [A_1{=}0 \wedge B_1{=}0 \wedge C_1{=}0]. \tag{51}$$

Next, we note that if a logical tautology can be expressed as

$$[E_0] \implies [E_1] \vee \ldots \vee [E_n], \tag{52}$$

then by applying the union bound (which asserts that the probability of at least one of a set of events occuring is no greater than the sum of the probabilities of each event occuring), one obtains

$$P(E_0) \leq \sum_{j=1}^{n} P(E_j). \tag{53}$$

Applying the union bound to Eq. (51) in particular yields

$$P_{A_2B_2C_2}(\mathbf{111}) \leq P_{A_1B_1C_1}(000) + P_{A_1B_2}(\mathbf{11}) + P_{B_1C_2}(\mathbf{11}) + P_{A_2C_1}(\mathbf{11}), \tag{54}$$

which is a constraint on the marginal *distributions*.

Note that this inequality allows one to demonstrate the incompatibility of the marginal distributions of Eqs. (15-17) with the spiral inflation of the Triangle scenario just as easily as one can with the tautology of Eq. (50). It suffices to note that the given distribution and causal structure imply that the left-hand side has nonzero probability (which

corresponds to the consequent of Eq. (50) being false) while every term on the right-hand side has zero probability (which corresponds to the antecedent of Eq. (50) begin true). But, of course, the inequality can witness many other incompatibilities in addition to this one.

As another example, consider the marginal problem where the variables are $\{A, B, C\}$, with each being binary, and the contexts are the pairs $\{AB\}$, $\{AC\}$, and $\{BC\}$. The following tautology provides a constraint on marginal deterministic assignments:

$$[\mathbf{A{=}1}, \mathbf{C{=}1}] \implies [\mathbf{A{=}1}, B{=}1] \vee [B{=}0, \mathbf{C{=}1}]. \tag{55}$$

(To see that this is a tautology, simply note that $E \wedge F \implies E \wedge F \wedge (G \vee \neg G) = (E \wedge F \wedge G) \vee (E \wedge F \wedge \neg G) \implies (E \wedge G) \vee (F \wedge \neg G)$.) Applying the union bound, one obtains the following constraint on marginal distributions[19]

$$P_{AC}(\mathbf{11}) \leq P_{AB}(11) + P_{BC}(\mathbf{01}). \tag{56}$$

In this section, we seek to determine, for any marginal scenario, the set of *all* inequalities that can be derived in this manner. We do so by **enumerating** the full set of constraints on marginal deterministic assignments for the given marginal scenario.

We outline the general procedure using the marginal scenario of Fig. 15, where the full set of variables is $\{A_1, A_2, B_1, B_2, C_1, C_2\}$ and the contexts are $\{A_1B_1C_1\}$, $\{A_1B_2C_2\}$, $\{A_2B_1C_2\}$, $\{A_2B_2C_1\}$ and $\{A_2B_2C_2\}$, pursuant to Eq. (43). As before, we will express the constraints on marginal deterministic assignments as logical implications with a joint valuation of one of the contexts as the **antecedent** and a disjunction over contexts of joint valuations thereon as the **consequent**. In the following, we explain how to generate *all* such implications which are tight in the sense that the consequent is minimal, i.e., involves as few terms as possible in the disjunction.

First, we fix the antecedant by choosing some context and a joint valuation of its variables. In order to generate all contraints on marginal deterministic assignments, one will have to perform this procedure for *every* context as the antecedent and every choice of joint valuation thereof. For the sake of concreteness, we take the example of $[\mathbf{A_2{=}1}, \mathbf{B_2{=}1}, \mathbf{C_2{=}1}]$ as the antecedent. Each logical implication we consider is required to have the property that any variable that appears in both the antecendent and the consequent must be given the same value in both.

To formally determine all valid consequents, we first consider two hypergraphs. Hypegraphs can be represented as zero/one matrices: Let the rows correspond to nodes and the columns to hyperedges. The positions of the 1's indicates which nodes participate in which hyperedge.

Each node in the first hypergraph corresponds to a possible joint valuation of the variables in some particular context. The hyperedges in the first hypegraph correspond to every possible joint valuation of all the variables. A hyperedge (joint valuation on all variables) contains a node (joint valuation on the marginal contexts) iff the hyperedge is an extension of the node; for example the hyperedge $[A_1{=}0, \mathbf{A_2{=}1}, B_1{=}0, \mathbf{B_2{=}1}, C_1{=}1, \mathbf{C_2{=}1}]$ is an extension of the node $[A_1{=}0, \mathbf{B_2{=}1}, \mathbf{C_2{=}1}]$. In our example following Fig. 15, this initial hypergraph has $5 \cdot 2^3 = 40$ nodes and $2^6 = 64$ hyperedges. Indeed, in 0/1 matrix notation, this first hypegraph is precisely the marginal description matrix $\boldsymbol{M}$ introduced near Eq. (46).

The second hypergraph is a sub-hypergraph of the first one. We delete from the first hypergraph all nodes and hyperedges which contradict the outcomes supposed by the antecedent. For example, the node $[\mathbf{A_2{=}1}, \mathbf{B_2{=}0}, C_1{=}1]$ contradicts the antecedent $[\mathbf{A_2{=}1}, \mathbf{B_2{=}1}, \mathbf{C_2{=}1}]$. We also delete the node corresponding to the antecedent itself. In our example, this final resulting hypergraph has $2^3 + 3 \cdot 2^1 = 14$ nodes and $2^3 = 8$ hyperedges.

All valid (minimal) consequents are (minimal) **transversals** of this latter hypergraph. A transversal is a set of nodes which has the property that it intersects every hyperedge in at least one node. In order to get implications which are as tight as possible, it is sufficient to enumerate only the minimal transversals. Doing so is a well-studied problem in computer science with various natural reformulations and for which manifold algorithms have been developed [57].

In our example, it is not hard to check that the consequent of

$$\begin{aligned}[\mathbf{A_2{=}1}, \mathbf{B_2{=}1}, \mathbf{C_2{=}1}] \implies\ & [A_1{=}0, B_1{=}0, C_1{=}0] \vee [A_1{=}1, \mathbf{B_2{=}1}, \mathbf{C_2{=}1}] \\ & \vee [\mathbf{A_2{=}1}, B_1{=}1, \mathbf{C_2{=}1}] \vee [\mathbf{A_2{=}1}, \mathbf{B_2{=}1}, C_1{=}1]\end{aligned} \tag{57}$$

is such a minimal transversal: every assignment of values to all variables which extends the assignment on the left-hand side satisfies at least one of the terms on the right, but this ceases to hold as soon as one removes any one term on the right.

---

[19] This inequality is in fact equivalent to Eq. (29).

We convert these implications into inequalities in the usual way via the union bound (i.e., replacing "⇒" by "≤" at the level of probabilities and the disjunctions by sums). For example the constraint on marginal deterministic assignments Eq. (57) translates to the constraint on marginal distributions

$$P_{A_2B_2C_2}(\mathbf{111}) \leq P_{A_1B_1C_1}(000) + P_{A_1B_2C_2}(1\mathbf{11}) + P_{A_2B_1C_2}(1\mathbf{11}) + P_{A_2B_2C_1}(1\mathbf{11}). \tag{58}$$

Note that Eq. (58) is a strengthening of Eq. (54). Eq. (58) was used earlier in this article as the starting point of our third example of how to derive a causal compatibility inequality for the Triangle scenario, in Sec. III-C (see Eq. (37)). Because Eq. (57) is the progenitor of this inequality, it can be thought of as the progenitor of the causal compatibility inequality that one derives from it, namely, Eq. (40).

Inequalities on marginal distributions that one derives from hypergraph transversals are generally weaker than those that result from a complete solution of the marginal problem. Nevertheless, many Bell inequalities are of this form, the CHSH inequality among them [56]. So it seems that this method is still sufficiently powerful to generate plenty of interesting inequalities. At the same time, it should be significantly easier to perform in practice than the full-fledged linear (let alone nonlinear) quantifier elimination, even if one does it for every possible antecedent.

In conclusion, linear quantifier elimination is the preferable tool for deriving inequalities for the marginal problem whenever it is computationally tractable; but whenever it is not, then enumerating hypergraph transversals presents a good alternative.

V. FURTHER PROSPECTS FOR THE INFLATION TECHNIQUE

Corollary 5 states that any causal compatibility inequality on the injectable sets of an inflation DAG G' can be translated into a causal compatibility inequality on the original DAG G. Consequently any technique for deriving causal compatibility inequalities on G' can potentially be amplified by the inflation technique. As we discovered in Sec. IV, even weak constraints at the level of the inflated DAG can translate into strong constraints at the level of the original DAG. In the following two subsections, we consider two additional possibilities for constraints that might be exploited in this way to derive better inequalities.

A. Using *d*-separation relations of the inflated DAG

In Sec. IV, we considered deriving causal compatibility inequalities on the inflated DAG by taking valid inequalities for the marginal polytope on the pre-injectable sets of the inflated DAG, and then making of use the ancestral independences to factorize the joint distributions on the pre-injectable sets into those on the injectable sets.

It is natural to wonder whether one can sometimes make use of facts about the causal structure that go beyond ancestral independences. It is standard practice, when deriving compatibility conditions for a DAG, to make use of arbitrary d-separation relations among variables: if, in a given DAG, $\boldsymbol{X}$ and $\boldsymbol{Y}$ are d-separated[20] by $\boldsymbol{Z}$, then a distribution is compatible with that DAG only if it satisfies the conditional independence relation $\boldsymbol{X} \perp\!\!\!\perp \boldsymbol{Y}|\boldsymbol{Z}$. For $\boldsymbol{Z} = \emptyset$, this specializes to ancestral independence of $\boldsymbol{X}$ and $\boldsymbol{Y}$. Thus it is natural to ask: can the inflation technique also sensibly make use of other d-separation relations among sets of observed variables?

Every conditional independence relation $\boldsymbol{X} \perp\!\!\!\perp \boldsymbol{Y}|\boldsymbol{Z}$ can be expressed as a polynomial equation in terms of probabilities: while it is most commonly written as $P_{\boldsymbol{XY}|\boldsymbol{Z}}(\boldsymbol{xy}|\boldsymbol{z}) = P_{\boldsymbol{X}|\boldsymbol{Z}}(\boldsymbol{x}|\boldsymbol{z})P_{\boldsymbol{Y}|\boldsymbol{Z}}(\boldsymbol{y}|\boldsymbol{z})$ for all $\boldsymbol{x}$, $\boldsymbol{y}$, and $\boldsymbol{z}$, it can also be written in terms of unconditional probabilities, in which case it takes the form

$$\forall \boldsymbol{xyz} : P_{\boldsymbol{XYZ}}(\boldsymbol{xyz})P_{\boldsymbol{Z}}(\boldsymbol{z}) = P_{\boldsymbol{XZ}}(\boldsymbol{xz})P_{\boldsymbol{YZ}}(\boldsymbol{yz})$$

for all $\boldsymbol{x}$, $\boldsymbol{y}$, and $\boldsymbol{z}$. Such a nonlinear constraint can be incorporated as a further restriction on the joint distributions compatible with the inflated DAG, supplementing the basic constraints of nonnegativity of probabilities for the joint distribution of the observed variables and the constraints implied by ancestral independences.

For example, in the spiral inflation of the Triangle scenario (Fig. 3), A_1 and C_2 are d-separated by $\{A_2B_2\}$ (in addition to being ancestrally independent). Hence one can try to incorporate the constraint that

$$\forall a_1a_2b_2c_2 : P_{A_1A_2B_2C_2}(a_1a_2b_2c_2)P_{A_2B_2}(a_2b_2) = P_{A_1A_2B_2}(a_1a_2b_2)P_{A_2B_2C_2}(a_2b_2c_2) \tag{59}$$

[20] The notion of d-separation is treated at length in [1, 3, 11, 13], so we elect not to review it here.

Every probability that appears in such an equation, though not defined on an injectable set, can still be expressed as a marginal of the joint distribution over all observed variables. For instance, we can express $P_{A_2B_2}(a_2b_2)$ as

$$\forall a_2b_2 : \; P_{A_2B_2}(a_2b_2) = \sum\nolimits_{a_1b_1c_1c_2} P_{A_1A_2B_1B_2C_1C_2}(a_1a_2b_1b_2c_1c_2). \tag{60}$$

Upon substituting such relations into Eq. (59), one obtains a system of polynomial equations and inequalities in terms of the observable joint probabilities. We can then proceed as we did before, eliminating the unknowns $P_{A_1A_2B_1B_2C_1C_2}(a_1a_2b_1b_2c_1c_2)$ from this system. The additional difficulty now is that some the equations are nonlinear. This idea even applies to some ancestral independences between sets that are not pre-injectable: for example, $A_1A_2B_2 \perp\!\!\!\perp C_2$ is also guaranteed in the spiral inflation of the Triangle scenario (Fig. 3), and results in a polynomial equation closely related to Eq. (59).

Many modern computer algebra systems have functions capable of tackling nonlinear quantifier elimination symbolically[21]. Currently, however, it is generally not practical to perform nonlinear quantifier elimination on large polynomial systems with many parameters to be eliminated. It may help to exploit results on the concrete algebraic-geometric structure of these particular systems [58].

If one is seeking merely to assess the compatibility of a *given* distribution with the causal structure, then one can avoid the quantifier elimination problem and simply try and solve an existence problem: after substituting the values that the given distribution prescribes for the joint outcomes on pre-injectable sets into the polynomial system in terms of the unknown global joint probabilities, one must only determine whether that system has a solution. Most computer algebra systems can resolve such *satisfiability* questions quite easily[22].

It is also possible to use a mixed strategy of linear and nonlinear quantifier elimination, such as Chaves [6] advocates. The explicit results of [6] are directly causal implications of the *original* DAG, achieved by applying a mixed quantifier elimination strategy. Perhaps further causal compatibility inequalities will be derivable by applying such a mixed quantifier elimination strategy to inflation DAGs.

B. Using copy-index equivalence relations on the inflated DAG

By the definition of an inflated model (Definition 2), if two variables in the inflated DAG G' are copy-index-equivalent, $A_i \sim A_j$, then each depends on its parents in the same fashion as A depends on its parents in the original DAG G. Hence A_i and A_j have the same dependence on their parents. Formally, from $A_i \sim A$ and Eq. (5), we infer that $P_{A_i|\mathsf{Pa}_{G'}(A_i)} = P_{A|\mathsf{Pa}_G(A)}$, and similarly $P_{A_j|\mathsf{Pa}_{G'}(A_j)} = P_{A|\mathsf{Pa}_G(A)}$. These two equations imply that

$$P_{A_i|\mathsf{Pa}_{G'}(A_i)} = P_{A_j|\mathsf{Pa}_{G'}(A_j)}. \tag{61}$$

By the definition of inflation, the ancestral subgraphs of A_i and A_j are identical, and equations like Eq. (61) also hold for all their ancestors. We conclude that also the marginal distributions of A_i and A_j must be equal, $P_{A_i} = P_{A_j}$. More generally, it may be possible to find pairs of contexts in G' of any size such that constraints of the form of Eq. (61) imply that the marginal distributions on these two contexts must be equal.

For example, consider the pair of contexts $\{A_1A_2B_1\}$ and $\{A_1A_2B_2\}$ for the marginal scenario defined by the spiral inflation of the triangle scenario (Fig. 3). Neither of these two contexts is an injectable set. Nonetheless, because of Eq. (61), we can conclude that their marginal distributions coincide in any inflation model,

$$\forall aa'b : \; P_{A_1A_2B_1}(aa'b) = P_{A_1A_2B_2}(aa'b). \tag{62}$$

We can also conclude that in the inflation model these marginal distributions satisfy $P_{A_1A_2B_1} = P_{A_2A_1B_2}$—where now the order of A_1 and A_2 is opposite on the two sides of the equation—or equivalently,

$$\forall aa'b : \; P_{A_1A_2B_1}(aa'b) = P_{A_1A_2B_2}(a'ab). \tag{63}$$

These constraints entail that $P_{A_1A_2B_2}$ must be symmetric under exchange of A_1 and A_2, which in itself is another equation of the type above.

Parameters such as $P_{A_1A_2B_1}(a_1a_2b)$, $P_{A_1A_2B_2}(a_1a_2b)$ and $P_{A_1A_2}(a_1a_2)$ can each be expressed as sums of the $P_{A_1A_2B_1B_2C_1C_2}(a_1a_2b_1b_2c_1c_2)$, so that relations such as Eqs. (62,63) each constitute an additional equation that can be

---

[21] For example *Mathematica*™'s `Resolve` command, *Redlog*'s `rlposqe`, or *Maple*™'s `RepresentingQuantifierFreeFormula`.

[22] For example *Mathematica*™'s `Reduce`ExistsRealQ` function. Specialized satisfiability software such as SMT-LIB's `check-sat` [59] are particularly apt for this purpose.

added to the system of equalities and inequalities that constitute the starting point of the satisfiability problem (if one is seeking to test the compatibility of a given distribution with the inflated DAG) or the quantifier elimination problem (if one is seeking to derive causal compatibility inequalities for the inflated DAG). If any such additional constraints yield stronger constraints at the level of the inflated DAG, then they may translate into stronger constraints at the level of the original DAG.

The general problem of finding pairs of marginal contexts in the inflated DAG for which relations of copy-index-equivalence imply equality of the marginal distributions, and the conditions under which such equalities may yield tighter inequalities, are discussed in Appendix B.

C. Causal inference in quantum theory and in generalized probabilistic theories

Recent work has sought to explore quantum generalizations of the notion of a causal model, termed *quantum causal models* [13, 14, 29, 60, 61]. We sketch the definition used in [13]. The causal structures are still represented by DAGs, but now in a quantum causal model the outgoing edges of latent nodes carry physical systems. Thus each such edge must be labelled by a Hilbert space. Each latent node takes all its incoming information—represented by its observed parent variables together with the incoming physical systems—and turns it into outgoing information via a quantum channel. Similarly, an observed node takes all its incoming information and applies a joint measurement on its incoming physical system as well as some classical information processing resulting in an outcome for its associated variable. Root variables can be thought of as settings of preparation procedures, while terminal nodes often represent the outcomes of measurements that are used in an experiment on quantum systems. In most cases that are of interest to quantum foundations, this complicated definition of quantum causal model can be formulated in an equivalent form that does not require a distinction of two kinds of edges [14].

A quantum causal model is still ultimately in the service of explaining joint distributions over classical variables. The joint distribution of these variables is the only experimental data with which one can confront a given quantum causal model. The basic problem of causal inference for quantum causal models, therefore, concerns the compatibility of a joint distribution over observed classical variables with a given DAG when the model supplementing the DAG is quantum. If this happens, we say that the distribution is *quantumly compatible* with the DAG.

One motivation for studying quantum causal models is that they offer a new perspective on an old problem in the foundations of quantum theory: that of establishing precisely which of the principles of classical physics must be abandoned in quantum physics. It was noticed by Fritz [12] and Wood and Spekkens [11] that Bell's theorem [34] states that there are distributions on observed variables of the Bell DAG that are quantumly compatible but not classically compatible with the DAG. Moreover, these distributions cannot be explained by *any* causal structure while complying with the additional principle that conditional independences should not be fine-tuned [11], i.e., while demanding that any observed conditional independence should be accounted for by the DAG. These results suggest that quantum theory is perhaps best understood as revising our notions of the nature of unobserved entities, how one represents causal dependencies thereon and incomplete knowledge thereof, while nonetheless *preserving* the spirit of causality and the principle of no fine-tuning [60, 62, 63].

Another motivation for studying quantum causal models is a practical one. Violations of Bell inequalities have been shown to constitute resources for information processing [64–66]. Hence it seems plausible that the existence of distributions on other DAGs that are quantumly compatible but not classically compatible may have similar applications to information processing. For example, it has been shown that in addition to the Bell scenario, such a quantum-classical separation also exists in the bilocality scenario [30] and the Triangle scenario [12], and it is likely that many more DAGs with this property will be found. The hope is that on any DAG supporting a quantum-classical separation, some of the separating distributions may constitute a resource for information processing.

So for both foundational and practical reasons, there is a strong motivation to find examples of DAGs that exhibit a quantum-classical separation. However, this is by no means an easy task. The set of distributions that are quantumly compatible with a given DAG is actually very similar to the set of distributions that are classically compatible with that DAG [12, 13]. For example, both the classical and quantum sets respect all the conditional independence relations among observed nodes that are implied by the d-separation relations of the DAG [13], and entropic inequalities are only of very limited use [12, 67]. We hope that the inflation technique will provide better tools for finding such separations.

In addition to quantum generalizations of causal models, one can define generalizations for other operational theories that are neither classical nor quantum [13, 14]. Such generalizations are formalized using the framework of *generalized probabilistic theories* (GPTs) [68, 69], which is sufficiently general to describe any operational theory that makes statistical predictions about the outcomes of experiments and passes some basic sanity checks. Some constraints on compatibility can be proven to be *theory-independent* in that they apply not only to classical and quantum causal models, but to any kind of generalized probabilistic causal model [13]. For example, the classically-valid conditional independence relations implied between observed variables in a DAG are all also valid in the GPT framework. Another

example is the entropic monogamy inequality Eq. (36), which was proven in [13] to be GPT valid as well. These kinds of constraints are of interest because they clarify what any conceivable theory of physics must satisfy in a given causal scenario.

The essential element in deriving such constraints is to only make reference to the observed nodes, as done in [13]. In fact, we now understand the argument of [13] to be an instance of the inflation technique. Nonetheless, we have seen that the inflation technique often yields inequalities that hold for the *classical* notion of compatibility, but which have quantum and GPT violations, such as the Bell inequalities of Example 3 of Sec. III-B and Appendix F. In fact, inflation can be used to derive inequalities with quantum violations for the Triangle scenario as well [70].

So what distinguishes applications of the inflation technique that yield inequalities for GPT compatibility from those that yield inequalities for classical compatibility? The distinction rests on a structural feature of the inflated DAG:

Definition 6. *In $G' \in \mathsf{Inflations}[G]$, an **inflationary fan-out** is a latent node that has two or more children that are copy-index equivalent.*

The web and spiral inflations of the triangle DAG, depicted in Fig. 2 and Fig. 3 respectively,contain one or more inflationary fan-outs, as does the inflation of the Bell DAG that is depicted in Fig. 12. On the other hand, the simplest inflation of the triangle DAG that we consider in this article, the cut inflation depicted in Fig. 5, does not contain any inflationary fan-outs.

The inflation technique can only detect a GPT-classical separation if the inflation DAG has an inflationary fan-out. We now explain the intuition for why this is the case. In an inflation model, the copy-index-equivalent children of an inflationary fan-out causally depend on it in precisely the same way as their counterparts in the original DAG do. For example, this dependence may be such that these two children are exact *copies* of the inflationary fan-out. So when one tries to write down a quantum or GPT version of our notion of inflation model, one quickly runs into trouble: in quantum theory, the *no-broadcasting theorem* shows that such duplication is impossible in a strong sense [71], and an analogous theorem holds for GPTs [72]. This is why in the presence of an inflationary fan-out, one cannot expect our inequalities to hold in the quantum or GPT case, which is consistent with the fact that they often do have quantum and GPT violations.

On the other hand, for any inflation DAG that does not contain an inflationary fan-out, the notion of inflation model generalizes to the quantum case: one equips every latent node in G' with the same quantum channel that the corresponding node in G is labelled by, while possibly discarding the outgoing systems which leave the node on those edges that do not appear in G'. For observed nodes, one can likewise use the exact same data as on G. That these prescriptions make sense crucially rests on the assumption that G' is an inflation of G, so that the ancestries of any node in G' mirrors the ancestry of the corresponding node in G perfectly. Hence for inflation DAGs G' without inflationary fan-outs, we have quantum analogues of Lemma 3 and Corollary 5. The problem of quantum causal inference on G therefore translates into the corresponding problem on G', and any constraint that we can derive on G' translates back to G. In particular, our Examples 1, 4 and 5 also hold for quantum causal inference: perfect correlation is also quantumly incompatible with the Triangle scenario, and the inequalities Eqs. (32,36) have no quantum violations. All of the exact same statements apply likewise in the GPT case.

In the remainder of this section, we discuss the relation between the quantum and the GPT case. Since quantum theory is a particular generalized probabilistic theory, quantum compatibility trivially implies GPT compatibility. Through the work of Tsirelson [37] and Popescu and Rohrlich [38], it is known that the converse is not true: the Bell scenario manifests a GPT-quantum separation. The identification of distributions witnessing this difference, and the derivation of constraints on quantum compatibility with GPT violations, has been a focus of much foundational research in recent years. Traditionally, the foundational question has always been: why does quantum theory predict correlations that are *stronger* than one would expect classically? But now there is a new question being asked: why does quantum theory only allow correlations that are *weaker* than those predicted by other GPTs? There has been some interesting progress in identifying physical principles that can pick out the precise correlations that are exhibited by quantum theory [73–81]. Further opportunities for identifying such principles would be useful. This motivates the problem of classifying DAGs into those which have a quantum-classical separation, those which have a GPT-quantum separation and those which have both. Similarly, one can try to classify causal compatibility *inequalities* into those which are GPT-valid, those which are GPT-violable-but-quantum-valid, and those which are quantum-violable.

It may be possible to generalize the inflation technique to derive inequalities that can witness a GPT-quantum separation by finding a restricted notion of quantum causal model on inflation DAGs *with* inflationary fan-outs that would not apply to the GPT case. In quantum theory, there *are* linear maps that can achieve broadcasting [82], but these are not completely positive. Thus if one uses these to define the inflation of a quantum causal model, then some of the joint probabilities for observable nodes in the inflated DAG may end up being negative. Such inflations might still be useful as a mathematical tool for ultimately deriving causal compatibility inequalities on the original DAG, but one would need to proceed differently from the way we have proceeded in this article: whereas we have assumed that all joint outcomes on the inflated DAG have nonnegative probability, one could not impose such a constraint for the

type of quantum inflation just described. Instead, one could only demand nonnegativity for marginal distributions of collections of variables that do not include the children of an inflationary fan-out. The inflation DAG in such cases would not be physically realistic, but one could still interpret it as describing multiple different *counterfactual* scenarios within which the causal dependencies are the same.

An analysis along these lines has already been carried out successfully in the derivation of entropic inequalities that capture quantum compatibility. Namely, Chaves *et al.* [29] consider conditioning an observed variable on a "setting" variable, a structure that we would describe as an inflation DAG containing inflationary fan-outs. Chaves *et al.* [29] then take pains to avoid talking about a global joint distribution in any of the entropic inequalities they apply to this structure, precisely as we would want to do in constructing inequalities on our inflated DAG. In this way, they successfully derive entropic inequalities for quantum compatibility. So far, no inequalities polynomial in the probabilities have been derived using this method.

VI. CONCLUSIONS

We have described a new technique for deriving causal compatibility inequalities which we have termed the *inflation* technique. We have shown that many pre-existing techniques for witnessing incompatability and for deriving causal compatibility inequaities can be enhanced by the inflation technique. In particular, it can enhance existing methods regardless of whether these pertain to entropic quantitites, correlators or probabilities. Furthermore, we have shown how a complete or partial solution of the marginal problem for the pre-injectable sets of the inflated DAG can be leveraged to obtain causal compatibility inequalities for the original DAG. These inequalities are not necessarily linear in the probabilities for joint valuations of the observed variables, that is, they are typically nonlinear (i.e., polynomial) inequalities. As far as we can tell, our inequalities are not related to the nonlinear causal compatibility inequalities which have been derived specifically to constrain classical networks [19–21], nor to the nonlinear inequalities which account for interventions on a given causal structure [36, 83].

Because our technique is capable of exhibiting the incompatibility of the W-type distribution with the Triangle scenario, while entropic techniques cannot, it follows that our polynomial inequalities are stronger than entropic inequalities in at least some cases (see Example 2 of Sec. III-B).

A single causal structure has an unlimited number of potential inflations. Selecting a good inflation from which strong polynomial inequalities can be derived is an interesting challenge. To this end, it would be desirable to understand how particular features of the original causal structure are exposed when different nodes in the DAG are duplicated. By isolating which features are exposed in each inflation, we could conceivably quantify the utility for causal inference of each inflation. In so doing, we might find that inflated DAGs beyond a certain level of variable duplication need not be considered. The multiplicity beyond which further inflation is irrelevant may be related to the maximum degree of those polynomials which tightly characterize a causal scenario. Presently, however, it is not clear how to upper bound either number, or whether finite upper bounds can even be expected.

Causal compatibility inequalities are, by definition, merely *necessary* conditions for compatibility. For some DAGs, the inflation technique is able to derive sufficient conditions as well. This occurs for the Bell scenario, as noted in Appendix F. We currently do not know whether or not the inflation technique can be used to also obtain sufficient conditions for an arbitrary DAG (for instance, by applying the technique to all inflations of a DAG or some finite family of inflations). Some evidence against such sufficiency is that we have not seen a way to use the inflation technique to rederive Pearl's instrumental inequality.

We have described how the inflation technique can enhance the power of many diffferent techniques for deriving causal compatibility inequalities and witnessing incompatibility, by applying the latter technique to the inflated DAG and using Corollary 5 and Lemma 3. The computational difficulty of achieving this enhancement depends on the seed technique. We summarize the computational difficulty of various approaches in Tables I and II.

We have noted that some of the causal compatibility inequalities we derive by the inflation technique are necessary conditions not only for compatibility with a classical causal model, but also for compatibility with a causal model in *any* generalized probabilistic theory, which includes quantum causal models as a special case.

It would be enlightening to understand the extent to which our (classical) polynomial inequalities for a given DAG can be violated by a distribution arising in a quantum causal model for that DAG, that is, the extent to which our inequalities can exhibit a quantum-classical separation for DAGs other than the Bell scenario. A variety of techniques exist for estimating the amount by which a Bell inequality [95, 96] is violated in quantum theory, but even finding a quantum violation of one of our *polynomial* inequalities presents a new task for which we currently lack a systematic approach. Nevertheless, we know that there exists a difference between classical and quantum also beyond Bell scenarios [12, Theorem 2.16], and we hope that our polynomial inequalities will perform better in witnessing this difference than entropic inequalities do [13, 29].

Finally, we believe that it may be possible to generalize the inflation technique to derive inequalities that are

TABLE I. A comparison of different approaches for deriving constraints on compatibility at the level of the inflated DAG (which can then be translated into constraints on compatibility at the level of the original DAG).

Input from causal structure	General problem → Standard algorithm(s)		Difficulty
Only Ancestral independences among the observed variables	Marginal Problem [Sec. IV-D] i.e. Facet Enumeration	→ Fourier-Motzkin Elimination [84–88], Lexicographic Reverse Search [89]	Hard
	Finding Hardy-type tautologies (*partial* solution of marginal problem) [Sec. IV-E] i.e. identifying hypergraph transversals	→ see Eiter *et al.* [57]	Very easy
Ancestral independences among the observed variables + copy-index equivalence relations [Appendix B]	Linear quantifier elmination	→ Fourier-Motzkin Elimination [84–88], Equality set projection [90, 91]	Hard
All d-separation conditions on the observable variables [Sec. V-A]	Real Quantifier Elimination	→ Cylindrical Algebraic Decomposition, see [6]	Very hard

TABLE II. A comparison of different approaches for testing causal compatibility of a given distribution with a given DAG by means of using the inflated DAG. These approaches are all means of witnessing the incompatibility of a given distribution with the inflated DAG.

Input from causal structure	General problem → Standard algorithm(s)		Difficulty
Only ancestral independences among the observed variables without (or with) supplementary copy-index equivalence relations [Appendix B]	Linear Satisfiability of (supplemented) Marginal Problem [Sec. IV-C]	→ Simplex method [92, 93]	Very Easy
All d-separation conditions on the observable variables [Sec. V-A]	Nonlinear Satisfiability	→ See [59], and semidefinite relaxations [94]	Easy

necessary conditions for the compatibilty of a joint distribution over observed variables with a *quantum* causal model. This may provide an alternative approach to understanding the Tsirelson bound [10].

ACKNOWLEDGMENTS

E.W. would like to thank Rafael Chaves and T.C. Fraser for suggestions which have improved this manuscript. T.F. would like to thank Nihat Ay and Guido Montúfar for discussion and references. This research was supported in part by Perimeter Institute for Theoretical Physics. Research at Perimeter Institute is supported by the Government of Canada through the Department of Innovation, Science and Economic Development Canada and by the Province of Ontario through the Ministry of Research, Innovation and Science.

Appendix A: Algorithms for Solving the Marginal Problem

By solving the marginal problem, what we mean is to determine all the facets of the marginal polytope for a given marginal scenario. Since the vertices of this polytope are precisely the deterministic assignments of values to all variables, which are easy to enumerate, solving the marginal problem is an instance of a **facet enumeration problem**: given the vertices of a convex polytope, determine its facets. This is a well-studied problem in combinatorial optimization for which a variety of algorithms are available [97].

A generic facet enumeration problem takes a matrix of vertices $\boldsymbol{V} \in \mathbb{R}^{n\times d}$, where each row is a vertex, and asks what is the set of vectors $\boldsymbol{b} \in \mathbb{R}^d$ that can be written as a convex combination of the vertices using weights $\boldsymbol{x} \in \mathbb{R}^n$ that are nonnegative and normalized,

$$\left\{ \boldsymbol{b} \in \mathbb{R}^d \;\middle|\; \exists \boldsymbol{x} \in \mathbb{R}^n : \; \boldsymbol{b} = \boldsymbol{x}.\boldsymbol{V}, \;\; \boldsymbol{x} \geq \boldsymbol{0}, \;\; \sum_i x_i = 1 \right\}. \tag{A.1}$$

To solve the marginal problem one uses the transpose of the marginal description matrix introduced in Sec. IV-B as the input to the facet enumeration algorithm, i.e. $\boldsymbol{V} = \boldsymbol{M}^\top$, see Eq. (46).

The oldest-known method for facet enumeration relies on **linear quantifier elimination** in the form of Fourier-Motzkin (FM) elimination [84, 85]. This refers to the fact that one starts with the system $\boldsymbol{b} = \boldsymbol{x}.\boldsymbol{V}$, $\boldsymbol{x} \geq \boldsymbol{0}$ and $\sum_i x_i = 1$, which is the half-space representation of a convex polytope (a simplex), and then one needs to project onto $\boldsymbol{b}$-space by *eliminating* the variables $\boldsymbol{x}$ to which the existential *quantifier* $\exists \boldsymbol{x}$ refers. The Fourier-Motzkin algorithm is a particular method for performing this quantifier elimination one variable at a time; when applied to Eq. (A.1), it is equivalent to the *double description method* [85, 98]. Linear quantifier elimination routines are available in many software tools[23]. The authors found it convenient to custom-code a linear quantifier elimination routine in *Mathematica*™.

Other algorithms for facet enumeration that are not based on linear quantifier elimination include the following. *Lexicographic reverse search* (LRS) [89], which explores the entire polytope by repeatedly pivoting from one facet to an adjacent one, and is implemented in `lrs`. Equality Set Projection (ESP) [90, 91] is also based on pivoting from facet to facet, though its implementation is less stable[24]. These algorithms could be interesting to use in practice, since each pivoting step churns out a new facet; by contrast, Fourier-Motzkin type algorithms only generate the entire list of facets at once, after all the quantifiers have been eliminated one by one.

It may also be possible to exploit special features of marginal polytopes in order to facilitate their facet enumeration, such as their high degree of symmetry: permuting the outcomes of each variable maps the polytope to itself, which already generates a sizeable symmetry group, and oftentimes there are additional symmetries given by permuting some of the variables. This simplifies the problem of facet enumeration [100, 101], and it may be interesting to apply dedicated software[25] to the facet enumeration problem of marginal polytopes [102–104].

---

[23] For example *MATLAB*™'s `MPT2`/`MPT3`, *Maxima*'s `fourier_elim`, *lrs*'s `fourier`, or *Maple*™'s (v17+) `LinearSolve` and `Projection`. The efficiency of most of these software tools, however, drops off markedly when the dimension of the final projection is much smaller than the initial space of the inequalities. Fast facet enumeration aided by Chernikov rules [86, 99] is implemented in *cdd*, *PORTA*, *qskeleton*, and *skeleton*. In the authors experience *skeleton* seemed to be the most efficient. Additionally, the package *polymake* offers multiple algorithms as options for computing convex hulls.

[24] ESP [88, 90, 91] is supported by `MPT2` but not `MPT3`, and by the (undocumented) option of projection in the *polytope* (v0.1.2 2016-07-13) python module.

[25] Such as *PANDA*, *Polyhedral*, or *SymPol*. The authors found *SymPol* to be rather effective for some small test problems, using the options "`./sympol -a --cdd`".

Appendix B: Constraints on marginal distributions from copy-index equivalence relations

In Sec. V-B we noted that every copy of a variable in the inflated DAG has the same probabilistic dependence on its parents as every other copy (see Eq. (61)), and that it follows that for certain pairs of marginal contexts the marginal distributions are necessarily equal. In this section, we describe how to identify such pairs of contexts.

Given sets of nodes $\boldsymbol{U}$ and $\boldsymbol{V}$ in an inflated DAG G', let us say that a map $\varphi : \mathsf{SubDAG}(\boldsymbol{U}) \to \mathsf{SubDAG}(\boldsymbol{V})$ is a **copy isomorphism** if it is a graph isomorphism[26] between $\mathsf{SubDAG}(\boldsymbol{U})$ and $\mathsf{SubDAG}(\boldsymbol{V})$ such that $\varphi(X) \sim X$ for all $X \in \boldsymbol{U}$, meaning that φ maps every node $X \in \boldsymbol{U}$ to a node $\varphi(X) \in \boldsymbol{V}$ that is equivalent to X under dropping the copy index.

Furthermore, we say that a copy isomorphism on the subgraphs of the two contexts, $\varphi : \mathsf{SubDAG}(\boldsymbol{U}) \to \mathsf{SubDAG}(\boldsymbol{V})$, is an **inflationary isomorphism** whenever it can be extended to a copy isomorphism on their ancestral subgraphs of the two contexts, $\Phi : \mathsf{AnSubDAG}(\boldsymbol{U}) \to \mathsf{AnSubDAG}(\boldsymbol{V})$. Any copy isomorphism, Φ, on the ancestral subgraphs of the two contexts defines an inflationary isomorphism, φ, on the subgraphs of the two contexts by simply restricting the domain of Φ to $\mathsf{SubDAG}(\boldsymbol{U})$. So in practice, one can either start with $\varphi : \mathsf{SubDAG}(\boldsymbol{U}) \to \mathsf{SubDAG}(\boldsymbol{V})$ and try to extend it to $\Phi : \mathsf{AnSubDAG}(\boldsymbol{U}) \to \mathsf{AnSubDAG}(\boldsymbol{V})$, or start with such a Φ and see whether it restricts to a $\varphi : \mathsf{SubDAG}(\boldsymbol{U}) \to \mathsf{SubDAG}(\boldsymbol{V})$.

For a pair of contexts $\boldsymbol{U}$ and $\boldsymbol{V}$, a sufficient condition for equality of their marginal distributions in the inflation is that there exists an inflationary isomorphism between them. Because $\boldsymbol{U}$ and $\boldsymbol{V}$ might themselves contain several variables that are copy-index equivalent (recall the examples of Sec. V-B), it follows that in order to equate the distribution $P_{\boldsymbol{U}}$ with the distribution $P_{\boldsymbol{V}}$ in an unambiguous fashion, one needs to specify a correspondence between the variables that make up $\boldsymbol{U}$ and those that make up $\boldsymbol{V}$. This is exactly the data provided by the inflationary isomorphism φ. This result is summarized in the following lemma.

Lemma 7. *Let the DAG G' be an inflation of the DAG G, and let $\boldsymbol{U}$ and $\boldsymbol{V}$ be contexts in G' (not necessarily distinct). If there exists an inflationary isomorphism $\varphi : \mathsf{SubDAG}(\boldsymbol{U}) \to \mathsf{SubDAG}(\boldsymbol{V})$, then $P_{\boldsymbol{U}} = P_{\boldsymbol{V}=\varphi(\boldsymbol{U})}$ in every inflated causal model.*

Lemma 7 is best illustrated by returning to our example from Sec. V-B which considered the inflation DAG of Fig. 3 and the pair of contexts $\boldsymbol{U} = \{A_1A_2B_1\}$ and $\boldsymbol{V} = \{A_1A_2B_2\}$.

Consider the map

$$\varphi \;:\; A_1 \mapsto A_1, \qquad A_2 \mapsto A_2, \qquad B_1 \mapsto B_2 \tag{B.1}$$

One easily verifies that this is a copy isomorphism between $\mathsf{SubDAG}(\boldsymbol{U})$ and $\mathsf{SubDAG}(\boldsymbol{V})$ because it maps each variable in $\boldsymbol{U}$ to a variable in $\boldsymbol{V}$ that is equivalent up to copy-index and because it trivially implements a graph isomorphism (since neither of these graphs has any edges). There is a unique choice to extend φ to a copy isomorphism $\Phi : \mathsf{AnSubDAG}(\boldsymbol{U}) \to \mathsf{AnSubDAG}(\boldsymbol{V})$, namely, by having Φ reproduce the action of Eq. (B.1) and implement the following isomorphism between the ancestors

$$\Phi \;:\; X_1 \mapsto X_1, \qquad Y_1 \mapsto Y_1, \qquad Y_2 \mapsto Y_2, \qquad Z_1 \mapsto Z_2. \tag{B.2}$$

Therefore φ is indeed an inflationary isomorphism. From Lemma 7, we then conclude that any inflated model satisfies $P_{A_1A_2B_1} = P_{A_1A_2B_2}$.

Similarly, the map

$$\varphi' \;:\; A_1 \mapsto A_2, \qquad A_2 \mapsto A_1, \qquad B_1 \mapsto B_2 \tag{B.3}$$

is easily verified to be a copy isomorphism between $\mathsf{SubDAG}(\boldsymbol{U})$ and $\mathsf{SubDAG}(\boldsymbol{V})$, and there is again a unique choice to extend φ' to a copy isomorphism $\Phi' : \mathsf{AnSubDAG}(\boldsymbol{U}) \to \mathsf{AnSubDAG}(\boldsymbol{V})$, by extending Eq. (B.3) with

$$\Phi' \;:\; X_1 \mapsto X_1, \qquad Y_1 \mapsto Y_2, \qquad Y_2 \mapsto Y_1, \qquad Z_1 \mapsto Z_2, \tag{B.4}$$

so that φ' is verified to be an inflationary isomorphism. From Lemma 7, we then conclude that any inflated model also satisfies $P_{A_1A_2B_1} = P_{A_2A_1B_2}$. (And this in turn implies that for the context $\{A_1A_2\}$, the marginal distribution satisfies $P_{A_1A_2} = P_{A_2A_1}$.)

---

[26] A graph isomorphism is a bijective map between the nodes of one graph and the nodes of another, such that the action of the map transforms the complete *set of edges* defining the first graph into the complete set of edges comprising the second graph.

In order to avoid any possibility of conclusion, we emphasize that one does not infer constraints on the marginal distributions over $\boldsymbol{U}$ and $\boldsymbol{V}$ from the mere existence of a copy isomorphism between the subgraphs of $\boldsymbol{U}$ and $\boldsymbol{V}$ nor from the existence of a copy isomorphism between the ancestral subgraphs of $\boldsymbol{U}$ and $\boldsymbol{V}$. Rather, such constraints are inferred from the existence of an inflationary isomorphism between the subgraphs, i.e., the existence of a copy isomorphism between the ancestral subgraphs that restricts to a copy isomorphism between the subgraphs.

We emphasize this fact because it might seem, at first glance, that the existence of a copy isomorphism between ancestral subgraphs is *by itself* sufficient for deriving constraints on the marginal distributions. To see why this is not the case, we offer the following example.

Take as the original DAG the instrumental scenario of Pearl [22], and consider the inflation depicted in Fig. 17. Consider the pair of contexts $\boldsymbol{U} = \{X_1Y_2Z_1\}$ and $\boldsymbol{V} = \{X_1Y_2Z_2\}$ on the inflated DAG. Note that these are clearly not pre-injectable sets.

The ancestral subgraphs for these two contexts are precisely the same, namely the DAG of Fig. 18. This DAG has only the identity map as a graph isomorphism, and therefore this is the unique copy isomorphism between $\mathsf{AnSubDAG}\big(X_1Y_2Z_1\big)$ and $\mathsf{AnSubDAG}\big(X_1Y_2Z_2\big)$. But if we restrict the domain of this isomorphism to $\mathsf{SubDAG}\big(X_1Y_2Z_1\big)$, we clearly do *not* get an isomorphism between $\mathsf{SubDAG}\big(X_1Y_2Z_1\big)$ and $\mathsf{SubDAG}\big(X_1Y_2Z_2\big)$ because $Z_1 \mapsto Z_1$ and we require that $Z_1 \mapsto Z_2$. (In fact, there are no copy isomorphisms between $\mathsf{SubDAG}\big(X_1Y_2Z_1\big)$ and $\mathsf{SubDAG}\big(X_1Y_2Z_2\big)$ because there are no graph isomorphisms between $\mathsf{SubDAG}\big(X_1Y_2Z_1\big)$ and $\mathsf{SubDAG}\big(X_1Y_2Z_2\big)$.)

One can try to make use of Lemma 7 when deriving polynomial inequalities with inflation via solving the marginal problem, by imposing $P_{\boldsymbol{U}} = P_{\boldsymbol{\varphi(U)}}$ as an additional constraint for every inflationary isomorphism $\varphi : \mathsf{SubDAG}\big(\boldsymbol{U}\big) \to \mathsf{SubDAG}\big(\boldsymbol{V}\big)$ between sets of observable nodes. This is advantageous to speed up to the linear quantifier elimination, since one can solve each of the resulting equations for one of the unknown joint probabilities and thereby eliminate that probability directly without Fourier-Motzkin elimination.

Moreover, one could also hope that these additional equations would result in tighter constraints on the marginal problem, which would in turn yielder tighter causal compatibility inequalities. However, our computations have so far not revealed any example of such a tightening. In some cases, this lack of impact can be explained as follows. Suppose that $\varphi : \mathsf{SubDAG}\big(\boldsymbol{U}\big) \to \mathsf{SubDAG}\big(\boldsymbol{V}\big)$ is an inflationary isomorphism which is not just the restriction of a copy isomorphism between the ancestral subgraphs, but even the restriction of a copy automorphism $\Phi' : G' \to G'$ of the entire inflated DAG onto itself; in particular, this assumption implies that Φ' also restricts to a copy isomorphism $\Phi : \mathsf{AnSubDAG}\big(\boldsymbol{U}\big) \to \mathsf{AnSubDAG}\big(\boldsymbol{V}\big)$ between the ancestral subgraphs. In this case, the irrelevance of the additional constraint $P_{\boldsymbol{U}} = P_{\varphi(\boldsymbol{U})}$ to the marginal problem for inflated models can be explained by the following argument.

Suppose that some joint distribution $P_{\mathsf{ObservedNodes}[G']}$ solves the unconstrained marginal problem, i.e., without requiring $P_{\boldsymbol{U}} = P_{\varphi(\boldsymbol{U})}$. Now apply Φ' to the variables in $P_{\mathsf{ObservedNodes}[G']}$, switching the variables around, to generate a new distribution $P' = P_{\Phi'(\mathsf{ObservedNodes}[G'])}$. Because the set of marginal distributions that arise from inflated models is invariant under this switching of variables, we conclude that P' is also a solution to the unconstrained marginal problem. Taking the uniform mixture of P and P' is therefore still a solution of the unconstrained marginal problem. But this uniform mixture also satisfies the supplementary constraint $P_{\boldsymbol{U}} = P_{\varphi(\boldsymbol{U})}$. Hence the supplementary constraint is satisfiable automatically whenever the unconstrained marginal problem is solvable, which makes adding the constraint irrelevant.

Note that the argument does not apply if the inflationary isomorphism $\varphi : \boldsymbol{U} \to \boldsymbol{V}$ cannot be extended to a copy

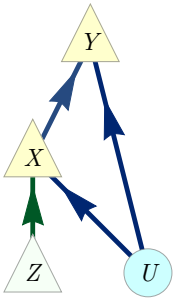

FIG. 16. The instrumental scenario of Pearl [22].

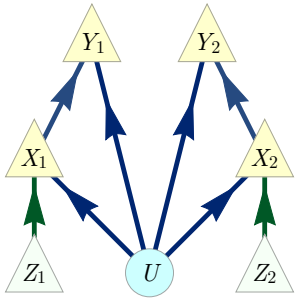

FIG. 17. An inflated DAG of the instrumental scenario which illustrates why coinciding ancestral subgraphs doesn't necessarily imply coinciding marginal distributions.

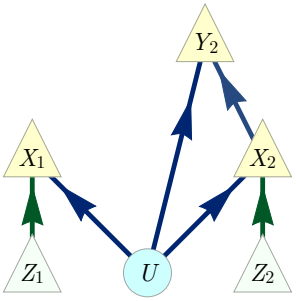

FIG. 18. The ancestral subgraph of Fig. 17 for either $\{X_1Y_2Z_1\}$ or $\{X_1Y_2Z_2\}$.

automorphism of the entire inflated DAG. It also does not apply if one uses the d-separation conditions beyond ancestral independence on the inflated DAG as additional constraints, because in this case the set of compatible distributions is not necessarily convex. In either of these cases, it is not apparent whether or not constraints arising from copy-index equivalence could yield tighter inequalities.

Appendix C: Using the Inflation Technqiue to Certify a DAG as "Interesting"

By considering all possible d-separation conditions implied by a given DAG, one can infer the set of all conditional independence (CI) relations that must hold in any joint distribution over the observed variables that is compatible with the given DAG. In the presence of nontrivial latent nodes, the set of all *observable* CI relations (that is, CI relations among observed variables) do not always exhaust the constraints on the joint distribution over the observed variables. Henson *et al.* [13] were concerned with identifying DAGs for which an observable distribution satisfying all observable CI relations is *not* a sufficient criterion for compatibility. They introduced the term **interesting** to refer to any DAG which exhibits a discrepancy between the set of observable distributions genuinely compatible with it and the set of observable distributions that merely reproduce its observable CI relations.

Henson *et al.* [13] derived novel necessary criteria on the structure of a DAG in order for it to be interesting, and they conjectured that their criteria may, in fact, be necessary and sufficient. As evidence in favour of this conjecture, they enumerated all possible DAGs with no more than six nodes satisfying their criteria. They found only 21 unique classes of potentially interesting DAGs. Of those 21, they further proved that 18 were unambiguously interesting by writing down an explicit incompatible distribution which nevertheless satisfied the DAGs observable CI relations. Incompatibility of the constructed distribution was certified by means of entropic inequalities.

That left three classes of DAGs as *potentially* interesting. For each of these, Henson *et al.* [13] derived all Shannon-type entropic inequalities in two different ways, once by accounting for non-observable CI relations (that is, CI relations that do not refer exclusively to observed variables) and once without. The existence of *novel* Shannon-type inequalities upon accounting for non-observable CI relations is evidence for the DAG being interesting. The only loophole is that perhaps those novel Shannon-type inequalities are actually non-novel non-Shannon-type inequalities implied by the observable CI relations alone [13].

One way to close this loophole would be to show that the novel Shannon-type inequalities imply constraints beyond some inner approximation to the genuine entropy cone absent non-observable CI relations, perhaps along the lines of Ref. [17]. Another is to use causal compatibility inequalities beyond entropic inequalities to identify some CI-respecting but incompatible distributions. Pienaar [26] accomplished precisely this, and should be credited with the original insight to explicitly consider the different values that an observable root variable might take. In the following, we demonstrate how the inflation technique can be used for this purpose. So far, we have only considered one of the three enigmatic causal structures, namely, Fig. 19.

The following representative causal compatibility inequalities for the DAG of Fig. 19 follow from the inflation technique applied to causal compatibility inequalities for the inflated DAG of Fig. 20, where the latter are obtained from Hardy-type tautologies as described in Sec. IV-E:

$$P_A(0)P_{ADE}(000) \leq P_{AE}(00)P_{AF}(00) + P_A(0)P_{ADF}(001), \tag{C.1}$$

$$P_A(0)P_{ADE}(100) \leq P_{AE}(10)P_{AF}(00) + P_A(1)P_{ADF}(001). \tag{C.2}$$

For example, the second inequality may be explicitly derived as follows. A Hardy-type tautology on the variables of the inflated DAG implies the following constraint on marginals:

$$P_{A_1A_2DE_2}(0100) \leq P_{A_1A_2F_1E_2}(0100) + P_{A_1A_2DF_1}(0101). \tag{C.3}$$

Applying factorization as per the ancestral independence relations of the inflated DAG, we obtain

$$P_{A_1}(0)P_{A_2DE_2}(100) \leq P_{A_1F_1}(01)P_{A_2E_2}(00) + P_{A_2}(1)P_{A_1DF_1}(001), \tag{C.4}$$

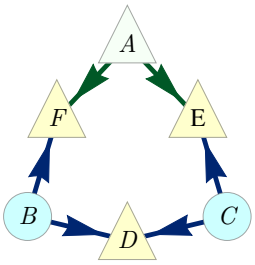

FIG. 19. DAG #15 in Ref. [13].

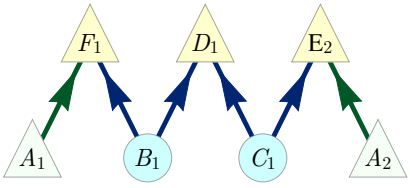

FIG. 20. A useful inflation of Fig. 19.

and finally translating this into a causal compatibility inequality on the original DAG using Corollary 5, we obtain Eq. (C.2).

In Pienaar [26], it was shown that the following distribution, which is easily verified to satisfy the CI relations among the observed variables of Fig. 19, namely, $A \perp\!\!\!\perp D$ and $E \perp\!\!\!\perp F|A$ [13], is nonetheless incompatible with Fig. 19:

$$P^{\text{Pien}}_{ADEF} := \frac{[0000] + [0101] + [1000] + [1110]}{4}, \quad \text{i.e.} \quad P^{\text{Pien}}_{ADEF}(adef) := \begin{cases} \frac{1}{4} & \text{if } e{=}a{\cdot}d \text{ and } f{=}(a{\oplus}1){\cdot}d, \\ 0 & \text{otherwise.} \end{cases} \tag{C.5}$$

It is easily verified that this distribution violates the causal incompatibility inequality of Eq. (C.2). It is in this sense that the inflation technique can show that the DAG of Fig. 19 is interesting.

There is another way to see that this distribution is not compatible with Eq. (C.2) using the inflation technique. First, one notes that any marginal distribution on DEF that is compatible with the DAG of Fig. 19 is necessarily also compatible the triangle scenario (where D, E and F are the observed variables). Second, one notes that the marginal distribution P^{Pien}_{DEF} is incompatible with the triangle scenario, since it violates inequality #8 of Sec. IV-D. This is the same inequality which rejects the W-distribution of Eq. (11). Like the W-distribution, the distribution P^{Pien} not only satisfies all Shannon-type entropic inequalities pertinent to Fig. 19, but lies within an inner approximation to the genuine entropy cone for that scenario[27]. In other words, there exists a distribution with the same joint and marginal entropies as P^{Pien} which *is* compatible with Fig. 19.

Finally, it may be worth noting that the inflation of Fig. 20 is precisely the "bilocality scenario" considered by Branciard *et al.* [30]. Therefore, the inflation technique permits us to translate every causal compatibility inequality for the bilocality scenario into a causal compatibility inequality for the DAG of Fig. 19.

[27] This is due to Weilenmann and Colbeck (private correspondence).

Appendix D: The Copy Lemma and Non-Shannon type Entropic Inequalities

As it turns out, the inflation technique is also useful outside of the problem of causal inference. As we argue in the following, inflation is secretly what underlies the **Copy Lemma** in the derivation of non-Shannon type entropic inequalities [105, Chapter 15]. The following formulation of the Copy Lemma is the one of Kaced [106].

Lemma 8. *Let A, B and C be random variables with distribution P_{ABC}. Then there exists a fourth random variable A' and joint distribution $P_{AA'BC}$ such that:*

1. $P_{AB} = P_{A'B}$,
2. $A' \perp\!\!\!\perp AC \mid B$.

The proof via inflation is as follows.

Proof. We begin by noting that every possible joint distribution P_{ABC} is compatible with a DAG of the form of Fig. 21. This follows from the fact that one may take X to be any **sufficient statistic** for the joint variable (A, C) given B, such as $X := (A, B, C)$. Next, we consider the inflation of Fig. 21 depicted in Fig. 22. The maximal injectable sets are $\{A_1B_1C_1\}$ and $\{A_2B_1\}$. By Lemma 3, because P_{ABC} is assumed to be compatible with Fig. 21, it follows that the marginals $\{P_{A_1B_1C_1}, P_{A_2B_1}\}$, where $P_{A_1B_1C_1} := P_{ABC}$ and $P_{A_2B_1} := P_{AB}$, are compatible with the inflated DAG of Fig. 22. The fact that A_2 is d-separated from A_1C_1 by B_1 in Fig. 22 implies that the joint distribution can be expressed as $P_{A_1A_2B_1C_1} := P_{A_1B_1C_1} \otimes P_{A_2B_1} \otimes P_{B_1}^{-1}$, which is only defined for those values of b_1 such that $P_{B_1}(b_1) \neq 0$. By construction, $P_{A_1A_2B_1C_1}$ has $P_{A_1B_1} = P_{A_2B_1} = P_{AB}$ and satisfies the conditional independence relation $A_2 \perp\!\!\!\perp A_1C_1 \mid B_1$. □

While it is also not hard to write down a distribution with the desired properties explicitly [105, Lemma 15.8], the fact that one can rederive it using the inflation technique is significant. For one, all the non-Shannon type inequalities derived by Dougherty *et al.* [107] are obtained by applying some Shannon type inequality to the distribution that is implied to exist by the Copy Lemma. Our result shows, therefore, that one can understand these non-Shannon type inequalities for a DAG as arising from Shannon-type inequalities applied to an inflation of the DAG. Indeed, it may be that the inflation technique may be a more general-purpose tool for deriving non-Shannon-type entropic inequalities. A natural direction for future research is to explore whether more sophisticated applications of the inflation technique might result in *new* examples of such inequalities.

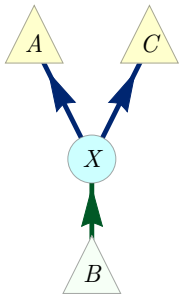

FIG. 21. A causal structure that is compatible with any distribution P_{ABC}.

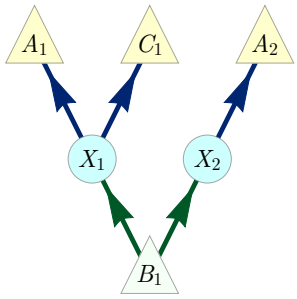

FIG. 22. An inflation of Fig. 21.

Appendix E: Causal compatibility inequalities for the Triangle scenario in machine-readable format

The following polynomial inequalities for the Triangle scenario with binary observed variables have been derived via the linear quantifier elimination method of Sec. IV using the inflated DAG of Fig. 3. Initially this has resulted in 64 symmetry classes of inequalities, where the symmetries are given by permuting the variables and inverting the outcomes. For the resulting 64 inequalities, numerical checks have found violations of only 37 of them: although they are all facets of the marginal polytope over the distributions on pre-injectable sets, there is no guarantee that they are also nontrivial inequalities at the level of the original DAG, and this has indeed turned out not to be the case for 26 of these symmetry classes of inequalities. Moreover, it is still likely to be the case that some of these inequalities are redundant; we have not yet checked whether for every inequality there is a distribution which violates the inequality but satisfies all others.

In the following table, the inequalities are listed in expectation-value form, where we assume the two possible outcomes of each variables to be $\{-1,+1\}$. Each row in the table gives the coefficients with one inequality, which is then ≥ 0. Inequalities $\#'s(1,3,4,8-17,19-24)$ in the table are also implied by the hypergraph transversals technique per Sec. IV-E.

TABLE III. List of inequalities as table of coefficients. This is a machine-readable version of the table in Sec. IV-D.

	constant	$\langle A\rangle$	$\langle B\rangle$	$\langle C\rangle$	$\langle AB\rangle$	$\langle AC\rangle$	$\langle BC\rangle$	$\langle ABC\rangle$	$\langle A\rangle\langle B\rangle$	$\langle A\rangle\langle C\rangle$	$\langle B\rangle\langle C\rangle$	$\langle C\rangle\langle AB\rangle$	$\langle B\rangle\langle AC\rangle$	$\langle A\rangle\langle BC\rangle$	$\langle A\rangle\langle B\rangle\langle C\rangle$
(#1):	1	0	0	0	1	1	0	0	0	0	1	0	0	0	0
(#2):	2	0	0	0	0	-2	0	0	0	0	0	-1	0	0	1
(#3):	3	1	-1	1	1	3	0	0	0	0	1	-1	-1	0	1
(#4):	3	1	-1	1	1	3	0	0	0	0	1	1	-1	0	-1
(#5):	3	0	1	0	1	0	-2	0	-1	1	0	1	-1	0	1
(#6):	3	0	1	0	0	-2	-2	0	0	1	0	-1	-1	0	1
(#7):	3	0	1	0	1	0	-2	0	1	-1	0	1	1	0	-1
(#8):	3	1	1	1	2	2	2	-1	1	1	1	1	1	1	-1
(#9):	3	1	1	1	0	2	-2	1	-1	1	1	1	1	-1	-1
(#10):	4	0	0	2	-2	-2	0	-1	2	0	2	1	1	1	0
(#11):	4	0	-2	0	-2	0	-3	1	0	0	1	1	-1	0	1
(#12):	4	0	-2	0	-2	-2	-3	1	0	2	1	1	1	0	-1
(#13):	4	0	0	0	2	-2	1	1	-2	-2	-1	-1	1	0	-1
(#14):	4	0	0	0	2	-2	1	1	-2	2	-1	1	1	0	1
(#15):	4	0	0	0	0	-2	3	1	0	2	1	-1	-1	0	1
(#16):	4	0	-2	0	-2	-2	-2	1	0	2	0	1	1	-1	0
(#17):	4	0	0	0	-2	-2	-2	1	2	2	2	1	1	1	0
(#18):	5	1	1	1	3	1	-4	0	-2	0	1	1	-1	0	1
(#19):	5	1	1	1	3	-1	-4	0	2	-2	1	1	1	0	-1
(#20):	5	1	-1	1	1	2	-2	-2	-2	-1	1	1	-2	-2	0
(#21):	5	1	1	1	1	2	-2	-1	0	-1	-1	2	1	1	-2
(#22):	5	-1	1	1	1	1	-1	1	-2	-2	2	-2	-2	-2	0
(#23):	5	1	1	1	2	1	-1	1	-1	0	2	-1	-2	-2	1
(#24):	5	1	1	1	-1	2	2	1	-2	-1	-1	2	1	-1	-2
(#25):	6	0	0	0	-4	-3	0	0	2	1	2	-2	-1	-2	1
(#26):	6	-2	0	2	-5	-3	0	0	1	1	0	-1	1	-2	2
(#27):	6	0	0	2	-4	3	0	0	2	1	0	-2	1	-2	1
(#28):	6	0	0	0	1	-3	2	0	1	1	-4	1	-1	-2	-2
(#29):	6	0	2	0	3	0	-5	0	1	-2	1	1	2	1	-2
(#30):	6	0	2	0	2	-2	1	0	-2	4	-1	2	2	1	1
(#31):	6	0	0	0	-2	-3	-2	-2	0	1	4	-2	-1	0	1
(#32):	7	1	1	1	2	1	-3	3	1	-2	2	3	2	-2	-1
(#33):	8	0	0	0	-2	-4	-2	-3	2	4	-2	-1	1	-3	2
(#34):	8	2	0	-2	-6	1	0	1	0	-1	2	1	2	-3	3
(#35):	8	2	0	0	6	1	-2	1	0	1	2	-1	-2	-3	3
(#36):	8	0	-2	-2	0	-6	1	1	2	0	-1	3	1	-2	-3
(#37):	8	0	2	0	1	2	-6	1	1	-2	0	2	3	-1	-3

Appendix F: Recovering the Bell inequalities from the inflation technique

To further illustrate the power of our inflated DAG approach, we now demonstrate how to recover all Bell inequalities [9, 10, 34] via our method. To keep things simple we only discuss the case of a bipartite Bell scenario with two values for both "settings" and "outcome" variables here, but the case of more parties and/or more values per variable is totally analogous.

The causal structure associated to the Bell [8–10, 34] experiment [13 (Fig. E#2), 11 (Fig. 19), 24 (Fig. 1), 14 (Fig. 1), 35 (Fig. 2b), 36 (Fig. 2)] is depicted here in Fig. 11. The observable variables are A, B, X, Y, and Λ is the latent common cause of A and B. In a Bell scenario, one traditionally works with the conditional distribution $P_{AB|XY}$, to be understood as an array of distributions indexed by the possible values of X and Y, instead of with the original distribution P_{ABXY}, which is what we do.

In the Bell scenario DAG, the maximal pre-injectable sets are

$$\begin{aligned}
&\{A_1B_1X_1X_2Y_1Y_2\}\\
&\{A_1B_2X_1X_2Y_2Y_2\}\\
&\{A_2B_1X_1X_2Y_2Y_2\}\\
&\{A_2B_2X_1X_2Y_2Y_2\},
\end{aligned} \tag{F.1}$$

where notably every maximal pre-injectable set contains all "settings" variables X_1 to Y_2. The marginal distributions on these pre-injectable sets are then specified by the original observable distribution via

$$\forall abx_1x_2y_1y_2: \begin{cases}
P_{A_1B_1X_1X_2Y_1Y_2}(abx_1x_2y_1y_2) = P_{ABXY}(abx_1y_1)P_X(x_2)P_Y(y_2),\\
P_{A_1B_2X_1X_2Y_1Y_2}(abx_1x_2y_1y_2) = P_{ABXY}(abx_1y_2)P_X(x_2)P_Y(y_1),\\
P_{A_2B_1X_1X_2Y_1Y_2}(abx_1x_2y_1y_2) = P_{ABXY}(abx_2y_1)P_X(x_1)P_Y(y_2),\\
P_{A_2B_2X_1X_2Y_1Y_2}(abx_1x_2y_1y_2) = P_{ABXY}(abx_2y_2)P_X(x_1)P_Y(y_1),\\
\qquad P_{X_1X_2Y_1Y_2}(x_1x_2y_1y_2) = P_X(x_1)P_X(x_2)P_Y(y_1)P_Y(y_2).
\end{cases} \tag{F.2}$$

By dividing each of the first four equations by the fifth, we obtain

$$\forall abx_1x_2y_1y_2: \begin{cases}
P_{A_1B_1|X_1X_2Y_1Y_2}(ab|x_1x_2y_1y_2) = P_{AB|XY}(ab|x_1y_1),\\
P_{A_1B_2|X_1X_2Y_1Y_2}(ab|x_1x_2y_1y_2) = P_{AB|XY}(ab|x_1y_2),\\
P_{A_2B_1|X_1X_2Y_1Y_2}(ab|x_1x_2y_1y_2) = P_{AB|XY}(ab|x_2y_1),\\
P_{A_2B_2|X_1X_2Y_1Y_2}(ab|x_1x_2y_1y_2) = P_{AB|XY}(ab|x_2y_2).
\end{cases} \tag{F.3}$$

The existence of a joint distribution over all six variables—i.e. the existence of a solution to the marginal problem—implies in particular

$$\forall abx_1x_2y_1y_2: \quad P_{A_1B_1|X_1X_2Y_1Y_2}(ab|x_1x_2y_1y_2) = \sum\nolimits_{a',b'} P_{A_1A_2B_1B_2X_1X_2Y_1Y_2}(aa'bb'|x_1x_2y_1y_2), \tag{F.4}$$

and similarly for the other three conditional distributions under consideration. For consistency with the causal hypothesis, therefore, the original distribution must satisfy in particular

$$\forall ab: \begin{cases}
P_{AB|XY}(ab|00) = \sum_{a',b'} P_{A_1A_2B_1B_2X_1X_2Y_1Y_2}(aa'bb'|0101)\\
P_{AB|XY}(ab|10) = \sum_{a',b'} P_{A_1A_2B_1B_2X_1X_2Y_1Y_2}(a'abb'|0101)\\
P_{AB|XY}(ab|01) = \sum_{a',b'} P_{A_1A_2B_1B_2X_1X_2Y_1Y_2}(aa'b'b|0101)\\
P_{AB|XY}(ab|11) = \sum_{a',b'} P_{A_1A_2B_1B_2X_1X_2Y_1Y_2}(a'ab'b|0101)
\end{cases} \tag{F.5}$$

The possibility to write the conditional probabilities in the Bell scenario in this form is equivalent to the existence of a latent variable model, as noted in Fine's Theorem [108]. Thus, if an inflated model exists with the required marginals, then a latent variable model of the original distribution exists as well (and conversely, trivially). Hence the inflated DAG of Fig. 12 provides necessary and sufficient conditions for the consistency of the original observed distribution with the Bell scenario causal structure.

Moreover, it is possible to describe the marginal polytope over the pre-injectable sets of Eq. (F.1), due to the fact that the "settings" variables X_1 to Y_4 occur in all four contexts. This description is easier to state for the marginal *cone*, by which we mean the convex cone spanned by the marginal polytope, i.e. the convex cone consisting of all

nonnegative linear combinations of deterministic assignments of values, or equivalently the convex cone of all measures on the set of joint outcomes. This cone lives in $\oplus_{i=1}^{4}\mathbb{R}^{2^6} = \oplus_{i=1}^{4}(\mathbb{R}^2)^{\otimes 6}$, where each tensor factor has basis vectors corresponding to the two possible outcomes of each variable, and the direct summands enumerate the four contexts. Now the marginal cone is precisely the set of all nonnegative linear combinations of the points

$$\begin{aligned}&(e_{A_1}\otimes e_{B_1}\otimes e_{X_1}\otimes e_{X_2}\otimes e_{Y_1}\otimes e_{Y_2})\\ \oplus\,&(e_{A_1}\otimes e_{B_2}\otimes e_{X_1}\otimes e_{X_2}\otimes e_{Y_1}\otimes e_{Y_2})\\ \oplus\,&(e_{A_2}\otimes e_{B_1}\otimes e_{X_1}\otimes e_{X_2}\otimes e_{Y_1}\otimes e_{Y_2})\\ \oplus\,&(e_{A_2}\otimes e_{B_2}\otimes e_{X_1}\otimes e_{X_2}\otimes e_{Y_1}\otimes e_{Y_2}),\end{aligned}$$

where all six variables range over their deterministic outcomes. Since the last four tensor factors occur in every direct summand in exactly the same way, the resulting marginal cone is linearly isomorphic to the cone generated by all vectors of the form

$$[(e_{A_1}\otimes e_{B_1})\oplus(e_{A_1}\otimes e_{B_2})\oplus(e_{A_2}\otimes e_{B_1})\oplus(e_{A_2}\otimes e_{B_2})]\otimes[e_{X_1}\otimes e_{X_2}\otimes e_{Y_1}\otimes e_{Y_2}]$$

in $\mathbb{R}^{2^2}\otimes\mathbb{R}^{2^4}$. Now since the first four variables in the first tensor factor vary completely independently of the latter four variables in the second tensor factor, the resulting cone will be precisely the tensor product [109] of two cones: first, the cone generated by all vectors of the form

$$(e_{A_1}\otimes e_{B_1})\oplus(e_{A_1}\otimes e_{B_2})\oplus(e_{A_2}\otimes e_{B_1})\oplus(e_{A_2}\otimes e_{B_2}),$$

and second the one spanned by all $e_{X_1}\otimes e_{X_2}\otimes e_{Y_1}\otimes e_{Y_2}$. While the latter cone is simply the standard positive cone of $\mathbb{R}^8$, the former cone is the cone generated by the "local polytope" or "Bell polytope" that is traditionally used in the context of Bell scenarios [10, Sec. II.B]. Standard results on tensor products of cones and polytopes [110] therefore imply that our marginal polytope is the tensor product of the Bell polytope, corresponding to the A_1 to B_2 part, with a simplex corresponding to the X_1 to Y_2 "settings" part. This implies that the facets of our marginal polytope are precisely the pairs consisting of a facet of the Bell polytope and a facet of the simplex. For example, in this way we obtain one version of the CHSH inequality as a facet of the marginal polytope,

$$\sum_{a,b,x,y}(-1)^{a+b+xy}P_{A_xB_yX_1X_2Y_1Y_2}(ab0101)\leq 2P_{X_1X_2Y_1Y_2}(0101).$$

Upon using Eq. (F.3), this becomes

$$\begin{aligned}\sum_{a,b}(-1)^{a+b}\big(&P_{ABXY}(ab00)P_X(1)P_Y(1)+P_{ABXY}(ab01)P_X(1)P_Y(0)\\ &+P_{ABXY}(ab10)P_X(0)P_Y(1)-P_{ABXY}(ab11)P_X(0)P_Y(0)\big)\leq P_X(0)P_X(1)P_Y(0)P_Y(1),\end{aligned}$$

so that dividing by the right-hand side results in essentially the conventional form of the CHSH inequality,

$$\sum_{a,b}(-1)^{a+b}\left(P_{AB|XY}(ab|00)+P_{AB|XY}(ab|01)+P_{AB|XY}(ab|10)-P_{AB|XY}(ab|11)\right)\leq 2.$$

In conclusion, the inflation technique is powerful enough to get a precise characterization of all distributions consistent with the Bell causal structure, and our technique for generating polynomial inequalities while solving the marginal problem recovers all Bell inequalities.

It is worth noting that the Bell inequalities may also be derived using the hypergraph-transversals / logical-tautologies technique discussed in Sec. IV-E. For example, the inequality

$$\begin{aligned}&P_{A_1B_1X_1Y_1}(1111)P_{X_2}(0)P_{Y_2}(0)\\ &\leq P_{A_1B_2X_1Y_2}(1010)P_{X_2}(0)P_{Y_1}(1)+P_{A_2B_1X_2Y_1}(0101)P_{X_1}(1)P_{Y_2}(0)+P_{A_2B_2X_2Y_2}(1100)P_{X_1}(1)P_{Y_1}(1)\end{aligned}\tag{F.6}$$

is a clear precursor of the Bell inequality

$$P_{AB|XY}(11|11)\leq P_{AB|XY}(10|10)+P_{AB|XY}(01|01)+P_{AB|XY}(11|00)\tag{F.7}$$

as Eq. (F.7) is obtained from Eq. (F.6) by dividing both sides by $P_{X_1Y_1X_2Y_2}(1100) = P_{X_1}(1)P_{Y_2}(1)P_{X_2}(0)P_{Y_2}(0)$ and then dropping copy indices. On the other hand, Eq. (F.6) follows directly from factorization of preinjectable sets and the tautology

$$\begin{aligned}&[\mathbf{A_1{=}1}, \mathbf{B_1{=}1}, \mathbf{X_1{=}1}, \mathbf{Y_1{=}1}, \mathbf{X_2{=}0}, \mathbf{Y_2{=}0}]\\ &\implies [\mathbf{A_1{=}1}, B_2{=}0, \mathbf{X_1{=}1}, \mathbf{Y_1{=}1}, \mathbf{X_2{=}0}, \mathbf{Y_2{=}0}] \vee [A_2{=}0, \mathbf{B_1{=}1}, \mathbf{X_1{=}1}, \mathbf{Y_1{=}1}, \mathbf{X_2{=}0}, \mathbf{Y_2{=}0}]\\ &\vee [A_2{=}1, B_2{=}1, \mathbf{X_1{=}1}, \mathbf{Y_1{=}1}, \mathbf{X_2{=}0}, \mathbf{Y_2{=}0}].\end{aligned} \tag{F.8}$$

[1] J. Pearl, *Causality: Models, Reasoning, and Inference* (Cambridge University Press, 2009).

[2] P. Spirtes, C. Glymour, and R. Scheines, *Causation, Prediction, and Search*, Lecture Notes in Statistics (Springer New York, 2011).

[3] M. Studený, *Probabilistic Conditional Independence Structures*, Information Science and Statistics (Springer London, 2005).

[4] D. Koller, *Probabilistic Graphical Models: Principles and Techniques* (MIT Press, Cambridge, MA, 2009).

[5] C. M. Lee and R. W. Spekkens, "Causal inference via algebraic geometry: necessary and sufficient conditions for the feasibility of discrete causal models," arXiv:1506.03880 (2015).

[6] R. Chaves, "Polynomial Bell inequalities," Phys. Rev. Lett. **116**, 010402 (2016).

[7] D. Rosset and N. Gisin, "Finite local models for all finite correlation scenarios," unpublished (2016).

[8] J. S. Bell, "On the Einstein-Podolsky-Rosen paradox," Physics **1**, 195 (1964).

[9] J. F. Clauser, M. A. Horne, A. Shimony, and R. A. Holt, "Proposed experiment to test local hidden-variable theories," Phys. Rev. Lett. **23**, 880 (1969).

[10] N. Brunner, D. Cavalcanti, S. Pironio, V. Scarani, and S. Wehner, "Bell nonlocality," Rev. Mod. Phys. **86**, 419 (2014).

[11] C. J. Wood and R. W. Spekkens, "The lesson of causal discovery algorithms for quantum correlations: causal explanations of Bell-inequality violations require fine-tuning," New J. Phys. **17**, 033002 (2015).

[12] T. Fritz, "Beyond Bell's theorem: correlation scenarios," New J. Phys. **14**, 103001 (2012).

[13] J. Henson, R. Lal, and M. F. Pusey, "Theory-independent limits on correlations from generalized Bayesian networks," New J. Phys. **16**, 113043 (2014).

[14] T. Fritz, "Beyond Bell's theorem II: Scenarios with arbitrary causal structure," Comm. Math. Phys. **341**, 391 (2015).

[15] R. Chaves and C. Budroni, "Entropic nonsignalling correlations," arXiv:1601.07555 (2015).

[16] R. Chaves, L. Luft, T. O. Maciel, D. Gross, D. Janzing, and B. Schölkopf, "Inferring latent structures via information inequalities," in *Proc. of the 30th Conference on Uncertainty in Artificial Intelligence* (AUAI, 2014) pp. 112–121.

[17] M. Weilenmann and R. Colbeck, "Non-Shannon inequalities in the entropy vector approach to causal structures," personal communication (2016).

[18] J. Åberg, R. Chaves, D. Gross, A. Kela, and K. U. von Prillwitz, "Inferring causal structures with covariance information," poster session, Quantum Networks conference (2016).

[19] A. Tavakoli, P. Skrzypczyk, D. Cavalcanti, and A. Acín, "Nonlocal correlations in the star-network configuration," Phys. Rev. A **90**, 062109 (2014).

[20] D. Rosset, C. Branciard, T. J. Barnea, G. Pütz, N. Brunner, and N. Gisin, "Nonlinear Bell inequalities tailored for quantum networks," Phys. Rev. Lett. **116**, 010403 (2016).

[21] A. Tavakoli, "Bell-type inequalities for arbitrary noncyclic networks," Phys. Rev. A **93**, 030101 (2016).

[22] J. Pearl, "On the testability of causal models with latent and instrumental variables," in *Proc. 11th Conference on Uncertainty in Artificial Intelligence*, AUAI (Morgan Kaufmann, San Francisco, CA, 1995) pp. 435–443.

[23] B. Steudel and N. Ay, "Information-theoretic inference of common ancestors," Entropy **17**, 2304 (2015).

[24] R. Chaves, L. Luft, and D. Gross, "Causal structures from entropic information: geometry and novel scenarios," New J. Phys. **16**, 043001 (2014).

[25] T. Fritz and R. Chaves, "Entropic inequalities and marginal problems," IEEE Trans. Info. Theo. **59**, 803 (2013).

[26] J. Pienaar, "Which causal scenarios are interesting?" arXiv:1606.07798 (2016).

[27] S. L. Braunstein and C. M. Caves, "Information-theoretic Bell inequalities," Phys. Rev. Lett. **61**, 662 (1988).

[28] B. W. Schumacher, "Information and quantum nonseparability," Phys. Rev. A **44**, 7047 (1991).

[29] R. Chaves, C. Majenz, and D. Gross, "Information–theoretic implications of quantum causal structures," Nat. Comm. **6**, 5766 (2015).

[30] C. Branciard, D. Rosset, N. Gisin, and S. Pironio, "Bilocal versus nonbilocal correlations in entanglement-swapping experiments," Phys. Rev. A **85**, 032119 (2012).

[31] W. Dür, G. Vidal, and J. I. Cirac, "Three qubits can be entangled in two inequivalent ways," Phys. Rev. A **62**, 062314 (2000).

[32] L. Hardy, "Nonlocality for two particles without inequalities for almost all entangled states," Phys. Rev. Lett. **71**, 1665 (1993).

[33] S. Mansfield and T. Fritz, "Hardy's non-locality paradox and possibilistic conditions for non-locality," Found. Phys. **42**, 709 (2012).

[34] J. S. Bell, "On the problem of hidden variables in quantum mechanics," Rev. Mod. Phys. **38**, 447 (1966).

[35] J. M. Donohue and E. Wolfe, "Identifying nonconvexity in the sets of limited-dimension quantum correlations," Phys. Rev. A **92**, 062120 (2015).

[36] G. V. Steeg and A. Galstyan, "A sequence of relaxations constraining hidden variable models," in *Proc. 27th Conference on Uncertainty in Artificial Intelligence* (AUAI, 2011) pp. 717–726.

[37] B. S. Cirel'son, "Quantum generalizations of Bell's inequality," Lett. Math. Phys. **4**, 93 (1980).

[38] S. Popescu and D. Rohrlich, "Quantum nonlocality as an axiom," Found. Phys. **24**, 379 (1994).

[39] J. Barrett and S. Pironio, "Popescu-rohrlich correlations as a unit of nonlocality," Phys. Rev. Lett. **95**, 140401 (2005).

[40] Y.-C. Liang, R. W. Spekkens, and H. M. Wiseman, "Specker's parable of the overprotective seer: A road to contextuality, nonlocality and complementarity," Phys. Rep. **506**, 1 (2011).

[41] D. Roberts, *Aspects of Quantum Non-Locality*, Ph.D. thesis, University of Bristol (2004).

[42] I. Pitowsky, "George Boole's 'conditions of possible experience' and the quantum puzzle," Br. J. Philos. Sci. **45**, 95 (1994).

[43] I. Pitowsky, *Quantum Probability - Quantum Logic*, Lecture Notes in Physics, Berlin Springer Verlag, Vol. 321 (Springer Berlin Heidelberg, 1989).

[44] H. G. Kellerer, "Verteilungsfunktionen mit gegebenen Marginalverteilungen," Z. Wahrscheinlichkeitstheorie **3**, 247 (1964).

[45] A. J. Leggett and A. Garg, "Quantum mechanics versus macroscopic realism: is the flux there when nobody looks?" Phys. Rev. Lett. **54**, 857 (1985).

[46] M. Araújo, M. Túlio Quintino, C. Budroni, M. Terra Cunha, and A. Cabello, "All noncontextuality inequalities for the n-cycle scenario," Phys. Rev. A **88**, 022118 (2013), arXiv:1206.3212.

[47] R. Horodecki, P. Horodecki, M. Horodecki, and K. Horodecki, "Quantum entanglement," Rev. Mod. Phys. **81**, 865 (2009).

[48] S. Abramsky and A. Brandenburger, "The sheaf-theoretic structure of non-locality and contextuality," New J. Phys. **13**, 113036 (2011).

[49] N. N. Vorob'ev, "Consistent families of measures and their extensions," Theory Probab. Appl. **7**, 147 (1960).

[50] T. Kahle, "Neighborliness of marginal polytopes," Beiträge Algebra Geom. **51**, 45 (2010).

[51] E. D. Andersen, "Certificates of primal or dual infeasibility in linear programming," Comp. Optim. Applic. **20**, 171 (2001).

[52] A. Garuccio, "Hardy's approach, Eberhard's inequality, and supplementary assumptions," Phys. Rev. A **52**, 2535 (1995).

[53] A. Cabello, "Bell's theorem with and without inequalities for the three-qubit Greenberger-Horne-Zeilinger and W states," Phys. Rev. A **65**, 032108 (2002).

[54] D. Braun and M.-S. Choi, "Hardy's test versus the Clauser-Horne-Shimony-Holt test of quantum nonlocality: Fundamental and practical aspects," Phys. Rev. A **78**, 032114 (2008).

[55] L. Mančinska and S. Wehner, "A unified view on Hardy's paradox and the Clauser–Horne–Shimony–Holt inequality," J. Phys. A **47**, 424027 (2014).

[56] G. Ghirardi and L. Marinatto, "Proofs of nonlocality without inequalities revisited," Phys. Lett. A **372**, 1982 (2008).

[57] T. Eiter, K. Makino, and G. Gottlob, "Computational aspects of monotone dualization: A brief survey," Discrete Appl. Math. **156**, 2035 (2008).

[58] L. D. Garcia, M. Stillman, and B. Sturmfels, "Algebraic geometry of Bayesian networks," J. Symbol. Comp. **39**, 331 (2003), arXiv:math/0301255.

[59] C. Barrett, P. Fontaine, and C. Tinelli, "The Satisfiability Modulo Theories Library (SMT-LIB)," `www.SMT-LIB.org` (2016).

[60] M. S. Leifer and R. W. Spekkens, "Towards a formulation of quantum theory as a causally neutral theory of Bayesian inference," Phys. Rev. A **88**, 052130 (2013).

[61] K. Ried, M. Agnew, L. Vermeyden, D. Janzing, R. W. Spekkens, and K. J. Resch, "A quantum advantage for inferring causal structure," Nature Physics **11**, 414 (2015).

[62] R. W. Spekkens, "The paradigm of kinematics and dynamics must yield to causal structure," *Questioning the Foundations of Physics: Which of Our Fundamental Assumptions Are Wrong?*, Questioning the Foundations of Physics , 5 (2015).

[63] J. Henson, "Causality, Bell's theorem, and Ontic Definiteness," arXiv:1102.2855 (2011).

[64] J. Barrett, N. Linden, S. Massar, S. Pironio, S. Popescu, and D. Roberts, "Nonlocal correlations as an information-theoretic resource," Phys. Rev. A **71**, 022101 (2005).

[65] V. Scarani, "The device-independent outlook on quantum physics," Acta Physica Slovaca **62**, 347 (2012).

[66] J.-D. Bancal, *On the Device-Independent Approach to Quantum Physics* (Springer International Publishing, 2014).

[67] R. Chaves and T. Fritz, "Entropic approach to local realism and noncontextuality," Phys. Rev. A **85**, 032113 (2012).

[68] H. Barnum and A. Wilce, "Post-classical probability theory," arXiv:1205.3833 (2012).

[69] P. Janotta and H. Hinrichsen, "Generalized probability theories: what determines the structure of quantum theory?" J. Phys. A **47**, 323001 (2014).

[70] T. C. Fraser and E. Wolfe, "Witnessing uniquely quantum correlations in the triangle scenario," unpublished (2016).

[71] H. Barnum, C. M. Caves, C. A. Fuchs, R. Jozsa, and B. Schumacher, "Noncommuting mixed states cannot be broadcast," Phys. Rev. Lett. **76**, 2818 (1996).

[72] H. Barnum, J. Barrett, M. Leifer, and A. Wilce, "Cloning and broadcasting in generic probabilistic theories," quant-ph/0611295 (2006).

[73] S. Popescu, "Nonlocality beyond quantum mechanics," Nat. Phys. **10**, 264 (2014).

[74] T. H. Yang, M. Navascués, L. Sheridan, and V. Scarani, "Quantum Bell inequalities from macroscopic locality," Phys. Rev. A **83**, 022105 (2011).

[75] D. Rohrlich, "Pr-box correlations have no classical limit," *Quantum Theory: A Two-Time Success Story: Yakir Aharonov Festschrift*, Yakir Aharonov Festschrift , 205 (2014).

[76] M. Pawlowski and V. Scarani, "Information Causality," arXiv:1112.1142 (2011).

[77] T. Fritz, A. B. Sainz, R. Augusiak, J. B. Brask, R. Chaves, A. Leverrier, and A. Acin, "Local Orthogonality as a Multipartite Principle for Quantum Correlations," Nat. Comm. **4**, 2263 (2013).

[78] A. B. Sainz, T. Fritz, R. Augusiak, J. B. Brask, R. Chaves, A. Leverrier, and A. Acín, "Exploring the Local Orthogonality Principle," Phys. Rev. A **89**, 032117 (2014).

[79] A. Cabello, "Simple explanation of the quantum limits of genuine n-body nonlocality," Phys. Rev. Lett. **114**, 220402 (2015).

[80] H. Barnum, M. P. Müller, and C. Ududec, "Higher-order interference and single-system postulates characterizing quantum theory," New Journal of Physics **16**, 123029 (2014).

[81] M. Navascués, Y. Guryanova, M. J. Hoban, and A. Acín, "Almost quantum correlations," Nat. Commun. **6**, 6288 (2015).

[82] B. Coecke and R. W. Spekkens, "Picturing classical and quantum Bayesian inference," Synthese **186**, 651 (2012).

[83] C. Kang and J. Tian, "Polynomial constraints in causal bayesian networks," in *Proc. of the 23rd Conference on Uncertainty in Artificial Intelligence* (AUAI, 2007) pp. 200–208.

[84] A. Fordan, *Projection in Constraint Logic Programming* (Ios Press, 1999).

[85] G. B. Dantzig and B. C. Eaves, "Fourier-Motzkin elimination and its dual," J. Combin. Th. A **14**, 288 (1973).

[86] S. I. Bastrakov and N. Y. Zolotykh, "Fast method for verifying Chernikov rules in Fourier-Motzkin elimination," Comp. Mat. & Math. Phys. **55**, 160 (2015).

[87] E. Balas, "Projection with a minimal system of inequalities," Comp. Optimiz. Applic. **10**, 189 (1998).

[88] C. N. Jones, E. C. Kerrigan, and J. M. Maciejowski, "On polyhedral projection and parametric programming," J. Optimiz. Theo. Applic. **138**, 207 (2008).

[89] D. Avis, "A revised implementation of the reverse search vertex enumeration algorithm," in *Polytopes — Combinatorics and Computation*, DMV Seminar, Vol. 29, edited by G. Kalai and G. M. Ziegler (Birkhäuser Basel, 2000) pp. 177–198.

[90] C. Jones, *Polyhedral Tools for Control*, Ph.D. thesis, University of Cambridge (2005).

[91] C. Jones, E. C. Kerrigan, and J. Maciejowski, *Equality set projection: A new algorithm for the projection of polytopes in halfspace representation*, Tech. Rep. (Cambridge University Engineering Dept, 2004).

[92] K. Korovin, N. Tsiskaridze, and A. Voronkov, "Implementing conflict resolution," Perspectives of Systems Informatics , 362 (2012).

[93] F. Bobot, S. Conchon, E. Contejean, M. Iguernelala, A. Mahboubi, A. Mebsout, and G. Melquiond, "A simplex-based extension of Fourier-Motzkin for solving linear integer arithmetic," Automated Reasoning , 67 (2012).

[94] M. Laurent and P. Rostalski, "The approach of moments for polynomial equations," in *Handbook on Semidefinite, Conic and Polynomial Optimization*, edited by M. F. Anjos and J. B. Lasserre (Springer, 2012) pp. 25–60.

[95] M. Navascués, S. Pironio, and A. Acín, "A convergent hierarchy of semidefinite programs characterizing the set of quantum correlations," New J. Phys. **10**, 073013 (2008).

[96] K. F. Pál and T. Vértesi, "Quantum bounds on bell inequalities," Phys. Rev. A **79**, 022120 (2009).

[97] D. Avis, D. Bremner, and R. Seidel, "How good are convex hull algorithms?" Computational Geometry **7**, 265 (1997).

[98] K. Fukuda and A. Prodon, "Double description method revisited," Combinatorics and Computer Science: 8th Franco-Japanese and 4th Franco-Chinese Conference , 91 (1996).

[99] D. V. Shapot and A. M. Lukatskii, "Solution building for arbitrary system of linear inequalities in an explicit form," Am. J. Comp. Math. **02**, 1 (2012).

[100] D. Bremner, M. Dutour Sikiric, and A. Schürmann, "Polyhedral representation conversion up to symmetries," in *Polyhedral computation*, CRM Proc. Lecture Notes, Vol. 48 (Amer. Math. Soc., 2009) pp. 45–71, arXiv:math/0702239.

[101] A. Schürmann, "Disc. geom. optim." (Springer International Publishing, Heidelberg, 2013) Chap. Exploiting Symmetries in Polyhedral Computations, pp. 265–278.

[102] V. Kaibel, L. Liberti, A. Schürmann, and R. Sotirov, "Mini-workshop: Exploiting symmetry in optimization," Oberwolfach Rep. , 2245 (2010).

[103] T. Rehn and A. Schürmann, "C++ tools for exploiting polyhedral symmetries," in *Proceedings of the Third International Congress Conference on Mathematical Software*, ICMS'10 (Springer-Verlag, Berlin, Heidelberg, 2010) pp. 295–298.

[104] S. Lörwald and G. Reinelt, "Panda: a software for polyhedral transformations," EURO Journal on Computational Optimization , 1 (2015).

[105] R. W. Yeung, *Information Theory and Network Coding* (Springer US, Boston, MA, 2008) Chap. Beyond Shannon-Type Inequalities, pp. 361–386.

[106] T. Kaced, "Equivalence of two proof techniques for non-Shannon-type inequalities," in *Information Theory Proceedings (ISIT)* (IEEE, 2013) pp. 236–240, arXiv:1302.2994.

[107] R. Dougherty, C. F. Freiling, and K. Zeger, "Non-Shannon information inequalities in four random variables," arXiv:1104.3602 (2011).

[108] A. Fine, "Hidden variables, joint probability, and the Bell inequalities," Phys. Rev. Lett. **48**, 291 (1982).

[109] I. Namioka and R. Phelps, "Tensor products of compact convex sets," Pacific J. Math. **31**, 469 (1969).

[110] T. Bogart, M. Contois, and J. Gubeladze, "Hom-polytopes," Math. Z. **273**, 1267 (2013), arXiv:1111.3880.